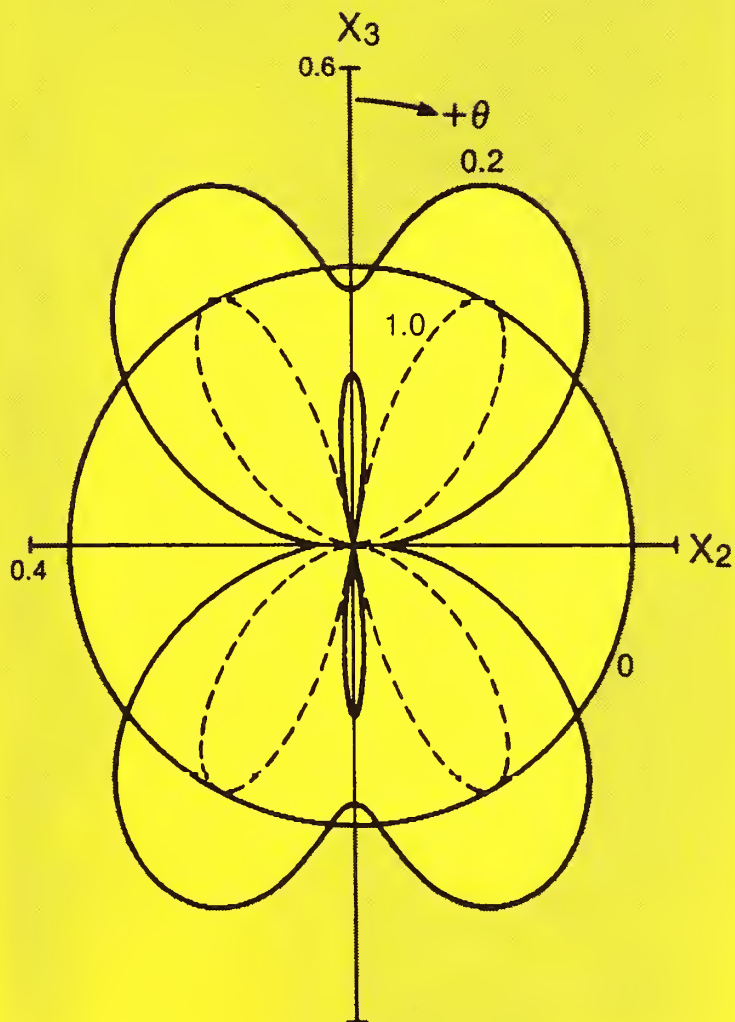


Institute for Materials Science and Engineering

# FRACTURE AND DEFORMATION

NAS-NRC  
Assessment Panel  
January 21-22, 1988

NBSIR 87-3613  
U.S. Department of Commerce  
National Bureau of Standards



Technical Activities  
1987



Institute for Materials Science and Engineering

# **FRACTURE AND DEFORMATION**

---

H.I. McHenry, Chief  
R.P. Reed, Chief until 9/1/87

NAS-NRC  
Assessment Panel  
January 21-22, 1988

NBSIR 87-3613  
U.S. Department of Commerce  
National Bureau of Standards  
October 1987

## **Technical Activities 1987**

For a uniaxial graphite-fiber-reinforced epoxy-matrix composite, this polar diagram shows the angular variation of the Poisson ratio  $\nu_{32}$ . It shows results for the matrix (0.0), a twenty-volume-percent composite (0.2), and the pure fiber (1.0). The dashed lines reflect negative values; in these directions, a tensile force would cause a transverse expansion.

Reported by R.D. Kriz and H.M. Ledbetter, "Elastic Representation Surfaces of Unidirectional Graphite/Epoxy Composites," in Recent Advances in Composites in the United States and Japan, ASTM STP 864, (Amer. Soc. Test. Mater., Phila., 1985), pp. 661-675.

## CONTENTS

INTRODUCTION . . . . .	1
RESEARCH STAFF . . . . .	3
TECHNICAL ACTIVITIES	
ELASTIC-PLASTIC FRACTURE MECHANICS . . . . .	7
Fracture Mechanics . . . . .	9
Nondestructive Evaluation . . . . .	16
Welding . . . . .	22
Thermomechanical Processing . . . . .	24
FRACTURE MECHANISMS AND ANALYSIS . . . . .	29
Physical Properties . . . . .	31
Fracture Physics . . . . .	34
Composite Mechanics . . . . .	36
Cryogenic Materials . . . . .	45
Material Performance . . . . .	50
OUTPUTS AND INTERACTIONS	
Selected Recent Publications . . . . .	53
Selected Technical and Professional Committee Leadership . . . . .	62
Industrial and Academic Interactions . . . . .	65
APPENDIX - ORGANIZATIONAL CHARTS	
National Bureau of Standards . . . . .	71
Institute for Materials Science and Engineering . . . . .	72



## DIVISION ORGANIZATION

Harry I. McHenry  
Chief (from 9/1/87)  
(303) 497-3268

Richard P. Reed  
Chief (until 9/1/87)  
(303) 497-3870

### ELASTIC-PLASTIC FRACTURE MECHANICS

Fracture Mechanics

David T. Read  
(303) 497-3853

Nondestructive Evaluation

Alfred V. Clark, Jr.  
(303) 497-3159

Welding

Thomas A. Siewert  
(303) 497-3523

Thermomechanical Processing

Yi-Wen Cheng  
(303) 497-5545

### FRACTURE MECHANISMS AND ANALYSIS

Fracture Physics

Ing-Hour Lin  
(303) 497-5791

Time-Dependent Properties

Richard J. Fields  
(301) 975-5712

Composite Mechanics

Ronald D. Kriz  
(303) 497-3547

Mechanical Metallurgy

George E. Hicho  
(301) 975-5707

Physical Properties

Hassel M. Ledbetter  
(303) 497-3443

Material Performance

Bruce W. Christ  
(303) 497-3424

Cryogenic Materials

Richard P. Reed  
(303) 497-3870

### ADMINISTRATIVE SUPPORT

Administrative Officer

Kathy Sherlock  
(303) 497-3288

Division Secretary

Heidi Mueller  
(303) 497-3251

Group Secretaries, Boulder

Virginia Candelaria  
(303) 497-5338

Chris King  
(303) 497-3290

Group Secretary, Gaithersburg

Judith Vaughan  
(301) 975-5704





# INTRODUCTION



Our division conducts research to expand knowledge of the deformation and fracture behavior of materials, mainly structural alloys, composites, and weldments. Other research is directed toward improving structural safety and industrial productivity. Research in fracture mechanics, nondestructive evaluation, and welding technology contributes to structural safety. The development of fitness-for-service criteria, quality control sensors, and deformation processing aids industrial productivity. Our research and technical activities respond to the diverse requirements of many sponsoring organizations:

- Base Program (STRS)
- NBS programs and initiatives
- Research for other governmental agencies
- Technical services

The base program supports the scientific base that underlies the division's goals to improve structural safety and industrial productivity. Research topics include nonlinear fracture mechanics, acoustoelasticity, arc physics, fracture physics, composite mechanics, and physical property modeling.

Current NBS programs and initiatives help us to respond to national needs. Recently, we have been working with the Office for Nondestructive Evaluation in applying our ultrasonics capabilities to the development of quality control sensors for monitoring formability of aluminum sheets. For the NBS Steel Initiative, we have used our simulation and control techniques to build a thermomechanical processing simulator, which is being used to study the physical metallurgy of high-strength steels during controlled rolling.

Research for other governmental agencies uses our technical resources to address division goals and benefit the nation:

Cryogenic Materials: Development and evaluation of materials for cryogenic service for DoE, NASA, and the Air Force.

Railway Safety: Use of nondestructive evaluation and fracture mechanics research on wheels and tank cars for the Federal Railway Administration.

Pressure Vessel Safety: Development of procedures for hazard recognition, assessment and mitigation for the Navy and for the Occupational Health and Safety Administration.

Nuclear Safety: Evaluation of the pressurized thermal shock resistance of steel plates through large-scale crack-arrest testing for the Nuclear Regulatory Commission.

In addition to our research programs, we provide technical services to many industrial, academic, and governmental organizations.

Testing Expertise: We assisted the MTS Corporation in setting up a cryogenic materials testing laboratory at the Société Européen Aérospatiale in France.

Failure Analysis: We investigated failures of power generation equipment for the Potomac Electric Power Company and of a ship-propulsion rotor for NOAA's Office of Marine Operations. We assisted Center for Building Technology in the investigations of the Moscow embassy and the Bridgeport, Connecticut building failure.

Test Services: We provide testing services in areas where we have exceptional capabilities, particularly measurements at cryogenic temperatures and mechanical tests in the 52-MN-load-capacity machine.

Consultation: In addition to routine interactions with governmental and private organizations, we provide in-depth consultation services to the U.S. Navy in the area of thermomechanical processing of steels, to the Occupational Health and Safety Administration regarding pressure vessel safety, and to several DoE, NASA, and DoD laboratories in the area of cryogenic materials.

This report provides a brief description of our research staff, technical activities, publications, and interactions. Our technical staff is interdisciplinary, evenly distributed among the materials, physics, and engineering disciplines. The technical activities are presented according to the NBS tasks assigned to our division: Elastic-Plastic Fracture Mechanics and Fracture Mechanisms and Analysis. The publications are another summary of the year's efforts. Leadership positions in professional committees are listed, and numerous industrial and academic interactions are briefly described.

H. I. McHenry  
Chief  
Fracture and Deformation Division

# RESEARCH STAFF



- |                       |   |
|-----------------------|---|
| Austin, Mark W.       | <ul style="list-style-type: none"> <li>• Elastic properties</li> <li>• X-ray diffraction applied to stacking-fault energy, internal strain, texture</li> </ul>  |
| Cheng, Yi-Wen         | <ul style="list-style-type: none"> <li>• Fatigue of metals</li> <li>• Fracture behavior of surface flaws</li> <li>• Fatigue-life predictions</li> <li>• Thermomechanical processing of steels</li> </ul>                                |
| Christ, Bruce W.      | <ul style="list-style-type: none"> <li>• Data-base management</li> <li>• Failure analysis of engineering structures</li> <li>• Mechanical properties of structural metals</li> <li>• Mechanical durability of motor vehicles</li> </ul> |
| Clark, Alfred V., Jr. | <ul style="list-style-type: none"> <li>• Theoretical and experimental ultrasonics</li> <li>• Engineering mechanics</li> <li>• Nondestructive evaluation</li> </ul>  |
| Delgado, Luz M.       | <ul style="list-style-type: none"> <li>• Mechanical testing</li> <li>• Compilation of low-temperature reference data</li> </ul>   |
| deWit, Roland         | <ul style="list-style-type: none"> <li>• Defect theory</li> <li>• Fracture mechanics</li> </ul>   |
| Fields, Richard J.    | <ul style="list-style-type: none"> <li>• Mechanical properties</li> <li>• High-temperature materials</li> </ul>   |
| Fitting, Dale W.      | <ul style="list-style-type: none"> <li>• Sensor arrays for NDE of anisotropic and inhomogeneous media</li> <li>• Ultrasonic and radiographic NDE</li> <li>• Signal and image processing</li> </ul>                                      |
| Heyliger, Paul R.     | <ul style="list-style-type: none"> <li>• Computational mechanics</li> <li>• Finite-element methods</li> <li>• Mechanics of composite materials</li> </ul>   |
| Hicho, George E.      | <ul style="list-style-type: none"> <li>• Mechanical metallurgy</li> <li>• Ferrous metallurgy</li> <li>• Failure analysis</li> <li>• Preparation and certification of standard reference materials</li> </ul>                            |
| Kim, Sudook           | <ul style="list-style-type: none"> <li>• Ultrasonic testing and analysis of elastic properties</li> <li>• Low-temperature physical properties</li> </ul>  |
| Kriz, Ronald D.       | <ul style="list-style-type: none"> <li>• Development of finite-element analysis for composites</li> <li>• Mechanics of composite materials</li> <li>• NDE of composite materials</li> </ul>   |

- |                      |  |
|----------------------|--|
| Ledbetter, Hassel M. | <ul style="list-style-type: none"> <li>• Physical properties of solids</li> <li>• Theory and measurement of elastic constants</li> <li>• Physical properties of austenitic steels</li> <li>• Measurement and modeling of physical properties of composite materials</li> <li>• Martensite-transformation theory</li> </ul> |
| Lin, Ing-Hour        | <ul style="list-style-type: none"> <li>• Fracture-toughening mechanisms</li> <li>• Ductile-brittle transition</li> <li>• Elastic interactions of cracks and defects</li> <li>• Dynamic deformation and fracture</li> <li>• Theory of dislocations and strengthening mechanisms</li> </ul>                                  |
| Low, Samuel R., III  | <ul style="list-style-type: none"> <li>• Mechanical testing</li> <li>• Instrumentation for dynamic measurements</li> </ul>   |
| McCowan, Chris N.    | <ul style="list-style-type: none"> <li>• Welding metallurgy</li> <li>• Mechanical properties at low temperatures</li> <li>• Metallography and fractography</li> </ul>  |
| McHenry, Harry I.    | <ul style="list-style-type: none"> <li>• Fracture mechanics</li> <li>• Low-temperature materials</li> <li>• Fracture control</li> </ul>  |
| Purtscher, Pat T.    | <ul style="list-style-type: none"> <li>• Fracture properties of high-strength steels</li> <li>• Metallography and fractography using light and electron microscopy</li> <li>• Mechanical and fracture toughness test methods</li> </ul>  |
| Read, David T.       | <ul style="list-style-type: none"> <li>• Physics of deformation and fracture</li> <li>• Elastic-plastic fracture mechanics, analysis and test methods</li> <li>• Mechanical properties of metals</li> </ul>  |
| Reed, Richard P.     | <ul style="list-style-type: none"> <li>• Mechanical properties</li> <li>• Low-temperature materials</li> <li>• Martensitic transformations</li> </ul>  |
| Reno, Robert C.      | <ul style="list-style-type: none"> <li>• Neutron diffraction studies of texture</li> <li>• Electron microscopy</li> <li>• Mössbauer spectroscopy</li> </ul>  |
| Schramm, Raymond E.  | <ul style="list-style-type: none"> <li>• Ultrasonic NDE of welds</li> <li>• Ultrasonic measurement of residual stress</li> <li>• Design of EMATs</li> </ul>  |
| Shepherd, Dominique  | <ul style="list-style-type: none"> <li>• Failure analysis</li> <li>• Metallography</li> <li>• Fractography</li> </ul>  |



- |                    |   |
|--------------------|---|
| Shives, T. Robert  | <ul style="list-style-type: none"><li>• Hardness test methods</li><li>• Mechanical properties</li><li>• Failure analysis</li></ul>  |
| Shull, Peter J.    | <ul style="list-style-type: none"><li>• Materials characterization with capacitive-array and eddy-current sensors</li><li>• Electronics for EMATs</li></ul>   |
| Siewert, Thomas A. | <ul style="list-style-type: none"><li>• Welding metallurgy of steel</li><li>• Gas-metal interactions during welding</li><li>• Welding data-base management</li></ul>  |
| Simon, Nancy J.    | <ul style="list-style-type: none"><li>• Information retrieval and data-base management of properties of materials at low temperatures</li><li>• Compilation of structural alloy properties at low temperatures for handbook</li></ul> |
| Tobler, Ralph L.   | <ul style="list-style-type: none"><li>• Fracture mechanics</li><li>• Fatigue crack growth resistance at low temperatures</li><li>• Low-temperature test standards</li></ul>   |
| Walsh, Robert P.   | <ul style="list-style-type: none"><li>• Mechanical properties at low temperatures</li><li>• Design and development of mechanical test equipment</li></ul>   |



# TECHNICAL ACTIVITIES



# ELASTIC-PLASTIC FRACTURE MECHANICS

This task addresses the establishment of a scientific basis for the development of fracture prevention requirements for structural materials. Safety and durability are primary considerations in the design and construction of engineering structures. Sophisticated methods to assess structural safety and durability have been developed on the basis of linear-elastic fracture mechanics. These analytical methods are applicable to the high-strength alloys used for aerospace vehicles and to the heavy-section steels used for nuclear pressure vessels. Unfortunately, the methods of linear-elastic fracture mechanics do not apply to a wide range of metal structures, including bridges, pressure vessels, ships, offshore structures, and pipelines, because in these applications, the materials of construction (typically steels and aluminum alloys) are highly plastic before fracture. Consequently, the assessments of their structural safety and durability are based on empirical methods and prior experience. Although current methods usually provide a reasonable record of structural safety, improved efficiency and productivity could be achieved if more rational methods were used to establish material-toughness requirements, allowable stress levels, minimum service temperatures, and weld-quality standards.

Over the years, we have expanded the scope of this task beyond the development of fracture mechanics models to evaluate the significance of flaws in materials. In 1980, we began research in nondestructive techniques to detect and size flaws and to measure residual stress, the largest uncertainties in the analysis of structural safety. In 1984, the task was expanded to include welding technology, because welds often have low fracture resistance, a high incidence of flaws, and high residual stress levels.

As the nation became more concerned about international competitiveness, we began to apply the technologies developed in this task to the improvement of industrial productivity. Using seed money from the Office of Nondestructive Evaluation, the steel initiative, and our base program, we are redirecting part of our resources as follows:

Thermomechanical Processing: The servohydraulic equipment, the computer-simulation and material-modeling capabilities, and the environmental controls developed for advanced fracture testing are being applied to research on the thermomechanical processing of steel.

Process Control Sensors: The sensor developments, the data-acquisition and signal-processing capabilities, and the acoustoelastic models developed for nondestructive evaluation are being applied to the development of process control sensors.

Welding Automation: The adaptive controls, the laser-imaging and video-processing capabilities, and the process models used to study the formation of weld defects are being applied to welding automation and process control.

## Representative Accomplishments

- In crack-arrest tests on nuclear pressure vessel steels, very large ( $10 \times 1 \times 0.15 \text{ m}^3$ ) single-edge-crack tensile plates had crack-arrest temperatures above the onset of upper shelf behavior. These data show a rapidly increasing arrest toughness with temperature and provide the technical basis to extend the ASME Section XI design curve to higher temperatures, the region of current engineering interest.
- A new model to describe plastic fracture of low-temperature alloys has been proposed. The fracture of austenitic steels has been examined at temperatures from 4 to 295 K in tensile and fracture toughness tests. A critical stress criterion for nucleation that depends on both the applied stress and strain accounts for the increase in fracture toughness with alloying and the dependence of fracture toughness on yield strength.
- Progress has been made in the application of electromagnetic-acoustic transducers (EMATs) to materials characterization and defect detection. EMATs have been fabricated and used to measure ultrasonic velocities in rolled aluminum-alloy sheet. These velocities correlated well with a measure of formability. In addition, construction is proceeding on two EMAT-based systems for field application. One system is designed for measurement of residual stress in the rims of railroad wheels; the other is intended for roll-by inspection of the treads of railroad wheels.
- A capacitive-array probe was designed, fabricated, and evaluated for use in materials characterization and nondestructive evaluation. The probe was used to characterize surface features (such as slots and steps) in dielectric and conducting media. Results were in good agreement with finite-element calculations, in which the probe's response to a flaw is computed using a line-integral technique. The probe had good sensitivity to artificial cracks in dielectric materials and to the thickness and porosity of thermal barrier coatings.
- The natural frequency for short-circuiting transfer in gas-metal-arc welding has been measured over a wide range of current and voltage. A stable current regulator was used to eliminate 60-Hz line ripple. The maximum frequency on the response surface corresponds to the empirically derived optimum weld condition now used in the welding industry. The existence of this natural frequency may be the basis for development of a control algorithm for closed-loop process control.
- A simulator has been built to study the thermomechanical processing of steels. Its features are: (1) vacuum to  $1 \times 10^{-5}$  torr, (2) deformation rate to 20 mm/mm/s, (3) load capacity of 250 kN, (4) cooling rate (using helium gas) to 25 K/s, (5) multiple-strike capability, and (6) a 450-kHz induction heater. The simulator is being used to develop improved procedures for controlled rolling and accelerated cooling of high-strength steels.

## Fracture Mechanics

D. T. Read, R. deWit, R. J. Fields, D. E. Harne, J. Heerens,\*  
S. R. Low III, J. D. McColskey, H. I. McHenry, P. T. Purtscher,  
R. P. Reed

Fracture mechanics relates the fracture resistance of a material containing a crack to the stress and strain fields in the vicinity of the crack. Fracture occurs when the crack-tip strain fields (the driving force for fracture) reach a magnitude that exceeds the material's resistance to fracture. Determination of the critical conditions is complicated by the numerous variables that influence the fracture process. Because modern structural metals are sufficiently tough that fracture rarely occurs under linear-elastic strain conditions, we have concentrated on fracture conditions of plastic strain at and near the crack tip.

Our research this past year can be categorized as studies of fracture driving force, material fracture resistance, and application of fracture mechanics to structural safety.

### **New testing facilities**

The new fracture testing laboratory is now operating. We have used the 1-MN machine for a wide-plate test in four-point bending. We have used the 100-kN machine for many fracture toughness tests, and a servo controller has been ordered for the 5-MN ( $1 \times 10^6$ -lbf) machine.

### **Driving force for fracture**

**Weldments with residual stresses.** The experimental technique of direct measurement of the J-integral was adapted to measure J during the cutting of a notch in a large, thick plate containing a weld in a groove. The groove weld simulated a repair weld in a pressure vessel (damage, such as pitting or cracking, found during inspection is repaired by grinding out and welding). The welded plate was instrumented with strain gages, and then the notch was cut with a special circular saw designed for minimum interference with the strain gages. After each increment of cut depth, the strain gages were scanned and the strain relaxations were recorded.

Analysis of the strain data to produce J-integral values had to be approximate because J is not path-independent when the path includes both base plate and weld metal. However, the measured relaxations of the strains on the back face of the specimen (opposite the notch) were small.

---

\*Guest worker from GKSS Research Center, Geesthacht, West Germany.



This result supported our assumption that the strain changes at the interface between the weld and base metal were also small. Thus, the change in the J-integral during the cutting of the notch could be calculated from the measured front- and back-face strains, after adjusting them for their initial value, which was the residual strain from welding. The results showed that the increase in the J-integral with crack depth was much larger in the as-welded plate than in the stress-relieved plate. With the mean of the yield strengths of the weld metal and the base plate used as the residual stress value, the measured J-integral compared reasonably well with values calculated for surface cracks in bending.

**Fracture mechanics analysis of weldments.** In the last two years, the effects of strength mismatch between weld metal and base plate were studied experimentally in tensile panels. This year, two efforts were made at modeling the results: the experimental results for surface flaws in two undermatched welds in tensile panels were compared with simple, closed-form predictive formulas; and finite-element analyses were performed on two-dimensional, center-cracked tensile panel configurations with mismatched welds.

The simplified line spring model was used to calculate the J-integral, and the modified critical COD model, the crack mouth opening displacement. Comparison of the calculations with experimental results showed that the general behavior was predicted properly by the models. The models also predict the effect of decreasing the weld yield strength, namely, a much higher crack driving force at constant applied stress level. However, the weldment behavior was far from elastic-perfectly plastic, as assumed by the models. The next modeling effort in these systems should include the strain-hardening effect, at least in the undermatched weld metal.

The finite-element analyses considered center-cracked tensile panels with small cracks (relative length, 0.017) and large cracks (relative length, 0.10). Each was analyzed with the weld undermatched by 20%, matched, and overmatched by 20%. Center-cracked panels were chosen to try to model the main features of the behavior economically, without concern for the three-dimensional complexities of surface cracks. The benefit of overmatching was greatest for the small cracks. The applied J-integral was reduced by up to a factor of 5 at strains several times yield and by a factor of 2 at yield strain. In the configurations with large cracks, the benefits of overmatching were much less, because the effect of the crack outweighed the benefits of overmatching, even though the overmatching was 20% and the crack was only 10% of the specimen width. Standard fracture toughness tests do not demonstrate the benefits of overmatching because the specimens have very deep cracks (relative size, 0.5). The driving force studies for the small cracks, however, show clearly that weld overmatching can be very beneficial.



**Finite-element analysis of surface cracks in tensile panels.** Three-dimensional elastic-plastic finite-element analysis of a fully instrumented test of a tensile panel with a small surface crack gave two significant results: (1) The direct experimental measurement of the J-integral for a surface flaw is approximately accurate, even though it cannot take into account the third-dimensional term that results from unmeasurable strains in the interior of the plate. The third-dimensional term accounts for only 15%, or less, of the total J-integral. (2) State-of-the-art finite-element analysis can predict the linear-elastic, ligament-yielding, and gross-section-yielding portions of the behavior of the specimen, but, so far, cannot predict the observed Lüders band effect. This study was done by R. H. Dodds, a professor at the University of Illinois, who worked with D. T. Read this past summer.

**Wide-plate crack-arrest testing.** We studied dynamic crack propagation and arrest in wide plates at temperatures up to the upper shelf region with the goal of predicting the behavior of a nuclear pressure vessel undergoing pressurized thermal shock.

Three groups of single-edge-cracked tensile specimens were scheduled for testing in a thermal gradient on the 26-MN universal testing machine at NBS. The first series of tests was on specimens of HSST A533 Grade B, Class 1, quenched-and-tempered steel. The second series of tests, now in progress, is on low upper-shelf 2½Cr-1Mo steel. A low upper-shelf weld material will be tested in the third series. Of the twenty-two tests scheduled, twelve have been completed. The edge-notched plates welded into the middle of the specimen were supplied by Oak Ridge National Laboratory. The pull plates and tabs were designed and constructed at NBS.

The thermal gradient in which the specimens are fractured extends from about -100 to 260°C (-150 to 500°F) across the 1-m specimen width. This is done so that the crack will initiate in a cold, brittle region and arrest in a hot, tough region. To establish this gradient, a heating and cooling system was constructed.

The test conditions, specimen configuration, and instrumentation used have been different for each test. Changes were made in attempts to obtain the desired crack-run and arrest behavior and to improve the quality of the data collected. In particular, efforts were made to initiate crack propagation at lower and lower stress-intensity factors. The results, which show a rapidly increasing arrest temperature, provide the technical basis for extending the ASME Section XI design curve to higher temperatures.

Each test yields a wealth of information. Strain gages were combined and located for the best determination of crack position as a function of time. The tape recorder enables recording 28 signals simultaneously. Of these, 20 were strain-gage signals; others were information about loads, crack mouth opening displacements, accelerometers, timing wires, and acoustic emission. Generally, these signals are recorded at 76 cm/s (30 in/s) over the half-hour period of loading until the specimen breaks in two. Hence, we have recorded signals with microsecond time resolution on about 300 m (1000 ft) of tape for each test.

The strain-gage data were analyzed to determine stress intensity as a function of crack position. This enabled evaluation of the crack-arrest toughness whenever the crack stopped. Since the crack arrested and reinitiated several times, crack arrest toughness values were obtained over a wide range of temperatures.

The analytical approach was to fit the measured strains to the mode-I crack-tip strain singularity, using stress intensity, crack length, and remote strain as fitting parameters. Despite the complexity of the test and the rather large distances between most of the strain gages and the crack tip at any given instant, the first term of the singularity represented the measured strains surprisingly well. The agreement between the form of the static, linear-elastic, singular, strain peak and the measured strain peak continued, even though strains several times yield were reached. The strains were definitely plastic because they were irreversible. A correction procedure was developed to relate the magnitude of the plastic strain peak to the stress-intensity factor through the use of the J-integral. The stress-intensity-factor values obtained concurred with handbook values. The measured strain peak was wider than the peak calculated by a static, elastic-plastic finite-element analysis. Thus, it appears that the linear-elastic singularity coincidentally describes the strains near a moving crack in an elastic-plastic material better than does the static, elastic-plastic singularity. These results show the importance of the extensive test instrumentation in enabling an understanding of the phenomena.

#### Material resistance to fracture

Fracture in the ductile-to-brittle transition region. The fracture toughness values of many steels in the ductile-to-brittle transition temperature range are considerably scattered. Values at the low end of the scatter band are so low that it is amazing that the steel structures providing the world's infrastructure survive so well. If the lower-bound toughness values were applied simultaneously with the largest credible cracks and stresses, failure would be predicted for many structures that have performed well for many years. This paradox can be considered to be an indictment of the usual fracture mechanics practice, which uses the worst-case conditions. The challenge is to learn how to account for the scatter in toughness values when assessing structural safety.

J. Heerens, a guest worker from GKSS Research Center, and D. T. Read investigated the reasons for the scatter of the fracture toughness in the transition region as well as the mechanisms leading to cleavage fracture. The test material was a quenched-and-tempered pressure-vessel steel, DIN 20 MnMoNi 55. The fracture surfaces of the specimens indicated that cleavage fracture starts at one small area in the ligament. Cleavage initiation occurs ahead of the crack tip at the location of the maximum normal stress. Fractography and metallography show four different types of initiation sites:

- Type A: Cleavage facet at the initiation site
- Type B: Unfractured inclusion at the initiation site
- Type C: Cluster of inclusions at the initiation site
- Type D: Initiation at a local zone of ductile tearing

In the fracture toughness specimens, cleavage crack initiation occurs at the location of maximum normal stress ahead of the crack tip. The scatter of fracture toughness values in the upper transition region is due to the scatter of  $r_c$ , the distance between the fatigue crack tip and the cleavage initiation site.

**New ductile fracture model.** Over the last fifteen years we have accumulated a considerable data base on the fracture toughness of austenitic stainless steels at 4 K. Our experience and understanding of these materials is now the foundation of attempts to relate toughness to inclusion spacing, interstitial contents, nickel content, and grain size. During the course of discussions of the effect of these material characteristics on toughness, the need for a mathematical-physical model became evident.

We have compared current theories\* for the micromechanisms of fracture and continuum mechanics with the results of our previous fracture mechanics tests on nitrogen-strengthened austenitic stainless steels at 4 K. These materials have a relatively high strength at this low temperature; nevertheless, they fracture in a ductile manner, retaining much of the high toughness that is characteristic of austenitic stainless steels at room temperature. Metallographic cross sections through the crack tip of tested fracture mechanics specimens revealed very limited regions of microscopic cracking in the plastic zones. Nucleation of microvoids occurs during the blunting stage of the fracture mechanics test at large plastic strains, and is limited to the region directly ahead of the advancing crack tip. It accounts for the majority of the energy absorbed in breaking the specimen.

We have developed a model that relates the stress-intensity factor for nucleation to the inclusion spacing, the critical stress for void nucleation, the material's strength, and the local stress at inclusions produced by dislocation pile-ups. The model assumes (1) nucleation of a microvoid is the critical step in the ductile fracture process, (2) void growth and coalescence occur with little or no additional applied energy, and (3) nucleation occurs when the interfacial stress between the inclusions and the matrix exceeds a critical value. This critical stress,  $\sigma_c$ , is composed of a macroscopic applied stress,  $\sigma_m$ , and a local stress,  $\sigma_\ell$ , that is a function of the applied strain,  $\epsilon$ :

$$\sigma_c = \sigma_\ell + \sigma_m$$

where  $\sigma_\ell = \sigma_H \epsilon^{\frac{1}{2}}$  and  $\sigma_H$  is a coefficient relating strain to stress near inclusions.

---

\*Theories of LeRoy, Embury, Edwards, and Ashby; Hutchinson; and Rice and Rosengren.

From the continuum mechanics analyses by Hutchinson, and Rice and Rosengren, we know the distribution of strain in the plastic zone ahead of the fatigue precrack. If we equate the strain at the point of nucleation in the fracture mechanics test to the assumed nucleation condition, we can solve for a stress-intensity factor for nucleation ( $K_{nuc}$ ):

$$K_{nuc} = \frac{\sigma_c - 3.5\sigma_y}{\sigma_H} (4.5\sigma_y EL)^{\frac{1}{2}}$$

where  $L$  is the average inclusion spacing,  $\sigma_y$  is the yield strength, and  $E$  is Young's modulus.

Using values for  $\sigma_c$  and  $\sigma_H$  estimated from exiting test results, we were able to calculate the effect of increasing the yield strength on the  $K_{nuc}$  of austenitic stainless steels at 4 K and to compare the prediction to the measured effect (see figure 1). The slope of the predicted curve and measured data match well for the higher strength levels ( $> 600$  MPa).

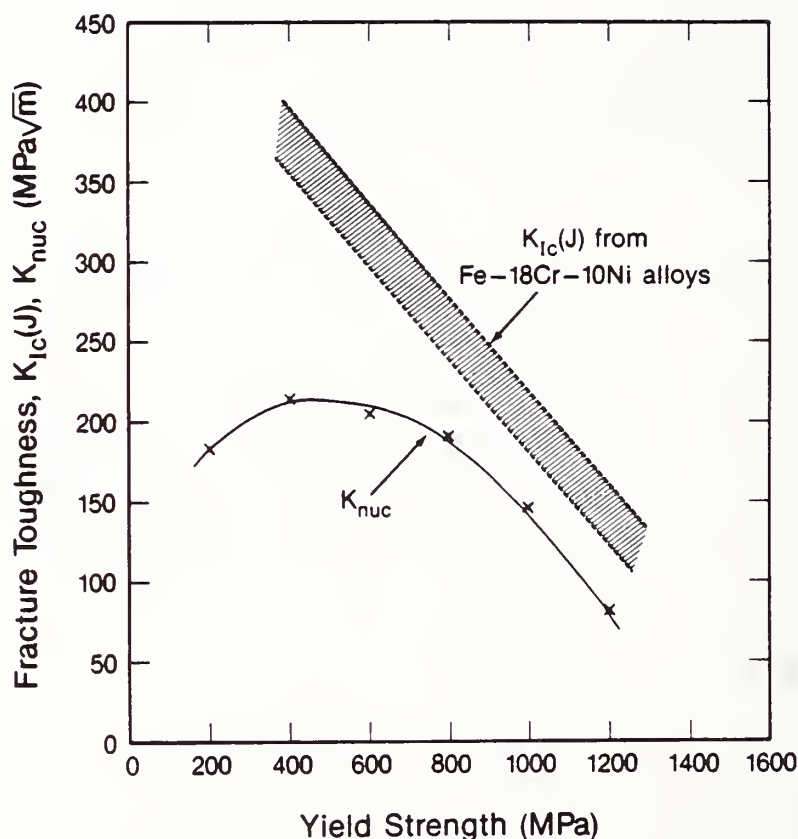


Figure 1. Measured and predicted dependence of fracture toughness on yield strength.



This indicates that the effect of yield strength on nucleation can account for the variation of fracture toughness with yield strength in the higher strength steels. At the lower stress levels ( $< 600$  MPa), the model predicts a smaller contribution of nucleation to the measured toughness. This agrees in principle with work done earlier on ductile fracture of low-strength materials, in which the fracture toughness is related to the growth of microvoids and the effect of nucleation is assumed to be negligible.

#### Application of fracture mechanics to repair welds of pressure vessels

Pressure vessels used for navy ship propulsion boilers and for civilian power plants are always given a post-weld heat-treatment (PWHT) after fabrication, to relieve residual stresses from welding and to improve the metallurgical properties of the weldment. Navy boilers are inspected and repaired repeatedly during their lifetimes, but PWHT of the repair welds is often difficult, time-consuming, and expensive. Therefore, the Navy has sponsored research into the benefits of PWHT after repair welding. An approach based on elastic-plastic fracture mechanics was used to determine and compare the crack-driving force in the PWHT condition and in the as-welded (AW) condition. Fracture toughness measurements were used to compare the material fracture resistance in the PWHT and AW conditions. Because we had both toughness and driving force data, we were able to calculate critical crack sizes in both the AW and PWHT condition. The results showed that the PWHT condition was definitely better because it could tolerate larger cracks. However, in the AW condition, cracks on the order of a few millimeters in depth could be tolerated. This approach seems to provide a means for making fitness-for-service decisions on PWHT, which in the past have been based on "engineering judgment."

## Nondestructive Evaluation

A. V. Clark, D. W. Fitting, P. R. Heyliger, D. V. Mitraković,\*  
J. C. Moulder, R. C. Reno, R. E. Schramm, P. J. Shull

Substantial progress has been made in application of electromagnetic-acoustic transducers (EMATs) to the practical problems of materials characterization and defect detection. EMATs are noncontacting devices (requiring no acoustic coupling); they use a transduction mechanism that is less efficient than conventional (piezoelectric) transducers. This low efficiency has limited the use of EMATs.

The signal-to-noise ratios of EMATs have been improved recently; in some cases, they approach the values of piezoelectric transducers. This improved performance is achieved through the use of high-current amplifiers and low-noise receivers designed and built chiefly by D. V. Mitraković, a guest worker from the University of Belgrade.

This improved EMAT system capability has been exploited in a number of projects: measurement of formability and texture, measurement of residual stress, and defect detection in railroad wheels.

### Ultrasonic measurement of texture and formability

In the project to measure formability, several sheets of commercial grade aluminum alloy (used as stock for beverage cans) were obtained from actual production runs. Data on formability of these sheets was provided by the manufacturer, with the condition that the proprietary nature of the material be respected.

The velocities of bulk and guided ultrasonic waves were measured by the NDE Group and others at NBS-Gaithersburg and Iowa State University who collaborated on this project. Measures of texture were calculated from the velocity measurements of each sheet. These calculations were based on recent theories that model the effect of texture on ultrasonic propagation. As a separate check on both the theoretical models and the ultrasonic measurements, the texture of the sheets was measured with neutron-diffraction pole figures made by R. C. Reno in Gaithersburg. Measures of texture, such as the quantity  $\omega_{420}$  shown in figure 2, obtained by the different methods were in good agreement.

As a practical matter, it is more significant that the ultrasonic determination of texture correlates with formability. The texture parameter  $\omega_{420}$ , as determined by EMAT measurement, correlated reasonably well with the formability, as shown in figure 3. The formability data were plotted in arbitrary units to protect the proprietary interest of the aluminum

---

\*Guest Worker from the University of Belgrade, Belgrade, Yugoslavia.

manufacturer. An elementary error analysis of the data of figure 3 revealed that the uncertainty is about the same as the uncertainty in the destructive measurements currently performed in production.

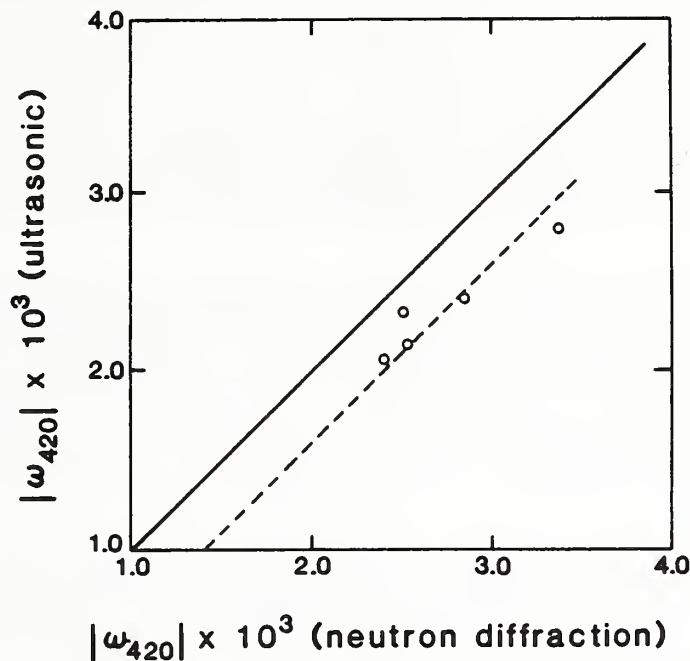


Figure 2. Comparison of ultrasonic and neutron-diffraction measurements of one texture parameter. If the data points agreed exactly, they would fall on the solid line. The broken line is the linear fit of the data.

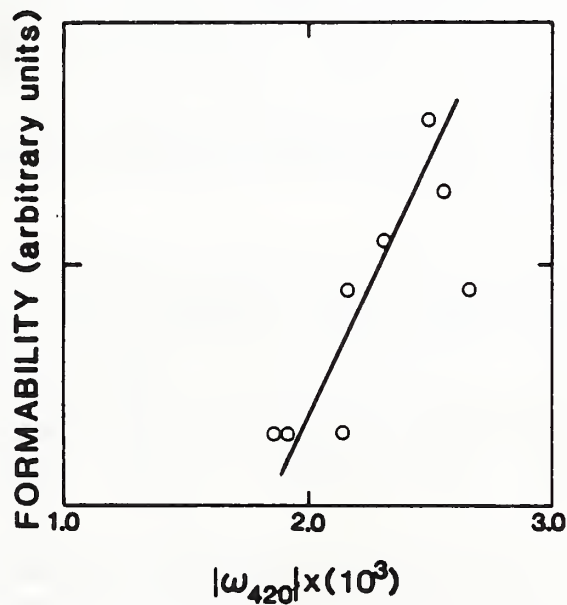


Figure 3. Comparison of the texture parameter with formability. The solid line is the linear fit of the data.

## EMAT inspection of railroad wheels

A new project has been initiated on use of EMATs for roll-by inspection of railroad wheels. The ultimate goal is construction of an EMAT system for use in a rail yard. For this application, an EMAT unit, consisting of a transmitter and receiver, would be mounted in a rail. As a wheel passes over the unit, ultrasonic signals would be generated by the EMAT transmitter. These signals, in the form of surface waves, will propagate around the tread of the wheel and be reflected by planar defects. The reflected signals will be detected by the receiving EMAT, amplified, and analyzed for features that correlate with defect size.

To date, several transmitting and receiving EMATs have been designed and tested for this purpose. For compactness, the transmitting and receiving EMATs have been integrated into a single search unit. The beam pattern of the acoustic wave generated by the transmitter has been characterized. A high-current pulser has been built to drive the transmitter at the frequency range of interest, and a low-noise amplifier has been constructed that gives about 80 dB of amplification of the microvolt-level signals detected by the receiving EMAT.

Tests have been performed on railroad wheels with artificial defects (saw cuts) in the treads. These defects have been detected by the search unit, with the unit mounted directly on the wheel and also with the unit mounted in a rail.

## Residual stress measurement with EMATs

To measure residual stress, shear waves are propagated through the stressed region, and the difference of arrival times of orthogonally polarized waves is measured. Since the effect of stress on ultrasonic velocity is small, it is necessary to measure arrival times with a precision of the order of 100 parts per million or better. This, in turn, requires a good signal-to-noise ratio (S/N) in the ultrasonic signals. The low S/N achievable with most EMAT systems has typically limited their use for measurement of stress in structural components.

With the new electronics, it has been possible to rapidly characterize the state of stress in thick steel components, such as welded plates and rims of railroad wheels. Residual stresses measured on 51-cm-thick welded steel plates were within 20 percent of the values determined by destructive methods using strain gages. The residual stress in a heat-treated railroad wheel subjected to drag-braking was also measured. The thickness-averaged stress was found to be compressive, a result verified by a saw-cutting procedure performed by the American Association of Railroads (AAR).

Further research is being done to obtain a method of quantitative residual stress determination in railroad wheels. If the method is successful, an EMAT-based system will be built and delivered to the Department of



Transportation Test Center (run under contract by the AAR). Then the system will undergo further testing by AAR researchers before being placed in service in a railroad-yard wheel shop.

### Capacitive-array sensor

A new type of NDE probe, a capacitive-array sensor, is being developed that is capable of operating on both dielectric and conductive materials. During the past year, work on the new probe included (1) design and characterization and (2) investigation of possible applications.

Unlike the eddy current or inductive probe, which responds to the interaction of the magnetic field with the workpiece, the capacitive-array probe interrogates the material with an electric field. Thus, it can interrogate surface features in conductive materials and both surface and subsurface features in dielectric materials.

To characterize the probe, we designed a series of tests on well-defined surface and subsurface flaws. Notches were cut on the surfaces of a conductor and an insulator; their depths ranged from 0.025 to 0.5 mm and their widths varied. The effects of notch width, lift-off, dielectric constant, sample grounding, and probe shielding were determined. The effects of notch depth as the probe scans the surface are shown in figure 4. A model was developed by P. R. Heyliger to predict and interpret these experimental results. Examples of the model's predictions for probe response to notches in a dielectric and in a conductor are shown in figure 5.

The response of the probe to subsurface flaws was determined on notches located from 0.3 to 4.0 mm below the surface (figure 6). The probe not only detected the flaws, but also small machining defects on the edges of the flaws 4.0 and 0.3 mm below the surface.

To determine the potential capabilities of this probe and the direction of this project in the future, we performed some preliminary studies of applications:

1. Ceramics - On 40- $\mu$ m-wide through cracks in alumina and 4.0- $\mu$ m-wide through cracks in glass, we observed variations in the signal response due to changes in thickness and porosity of thermal barrier coatings.
2. Dielectric constant monitoring - We observed two processes: the curing of five-minute epoxy and the recrystallization of phenolsolycelate.
3. Subsurface flaws in insulators - In plexiglass, we interrogated a flat, disc-shaped flaw that was 5 mm in diameter, 0.1 mm wide, and approximately 2 mm below the surface.

In these preliminary studies, the flaws or processes were clearly observed with signal-to-noise ratios greater than 10.



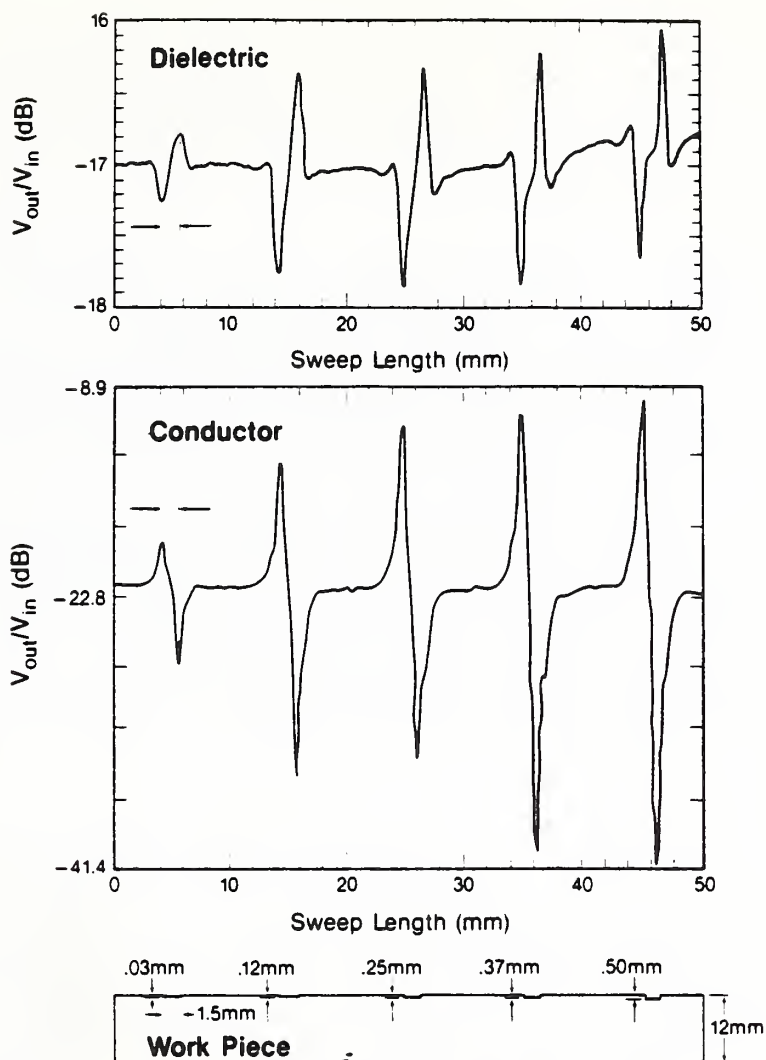


Figure 4. Response of the capacitive-array probe to a series of surface notches in a dielectric and a conductor.

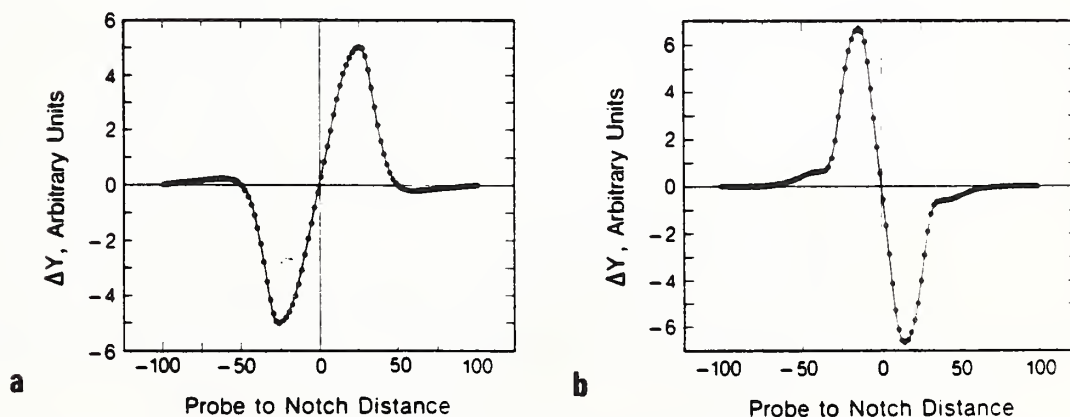


Figure 5. Calculated response of capacitive-array probe to a notch (a) in a dielectric (b) in a conductor.

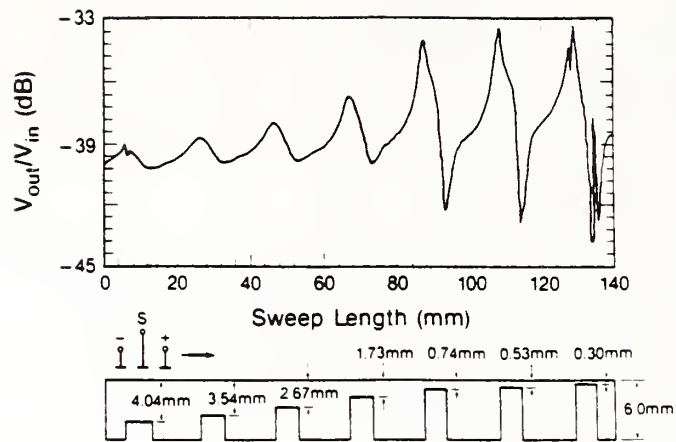


Figure 6. Response of the capacitive-array probe to subsurface notches in a dielectric.

## Welding

T. A. Siewert, C. N. McCowan, D. P. Vigliotti

### Arc physics

The natural arc frequency in short-circuiting transfer was mapped over a range of current and voltage, as shown in figure 7. Using the current regulator to filter the line frequency component, we were able to eliminate the problem that had prevented these data from being developed. The region of highest transfer frequency corresponds to the empirically derived optimum welding conditions that are now used in the welding industry. The existence of this natural frequency enables the development of an algorithm for closed-loop control of welding power sources.

The laser backlighting system and high-speed video camera were used to make precise ( $\pm 0.5$  mm) measurements of the arc length during spray transfer. These measurements, at a variety of current and voltage combinations (180 A, 27 V to 280 A, 30 V), are being used to refine the models for anode drop potential in the arc. The high-speed videos also reveal the gas flow patterns over the weld and the change in electrode shape as a function of current density.

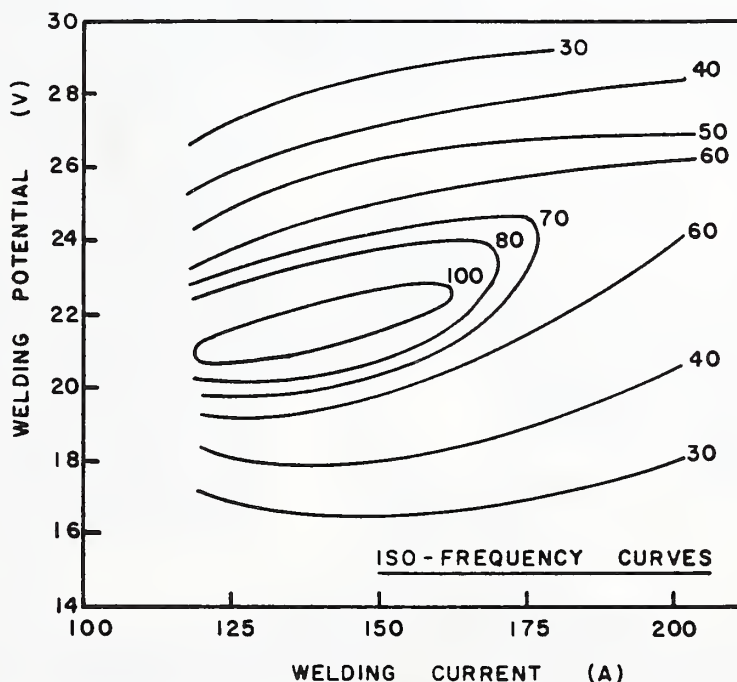


Figure 7. Map of natural arc frequency for short-circuiting droplet transfer.

Our exceptional laboratory facilities (current regulator, laser backlighting system, and high-speed video camera) continue to generate cooperative programs. During the past year, S. Liu of Pennsylvania State University and M. Shepard of Vanderbilt University have used our laboratory to study droplet transfer in gas-metal-arc (GMA) welding.

#### Stainless steel weldments

Our research indicated that inclusion spacing is the major cause of lower toughness in weldments than in base metal at cryogenic temperatures. To understand this effect better, two welds were evaluated. An experimental GMA electrode that had produced a weld with a strength of 1015 MPa and a fracture toughness of  $203 \text{ MPa}\cdot\text{m}^{1/2}$  at 4 K was used to produce the welds under conditions that minimize the oxygen content in welds. Instead of using a standard shielding gas tip with an Ar-2wt.%O<sub>2</sub> gas mix, a special tip was constructed to eliminate the aspiration of air into a 99.995-weight-percent pure argon atmosphere. The 50-percent reduction in weld oxygen concentration resulted in a weld with 40 percent better toughness ( $280 \text{ MPa}\cdot\text{m}^{1/2}$ ) at the same strength level (1000 MPa). The toughness of the welds produced substantially exceeded the goals of the U.S. fusion energy program ( $150 \text{ MPa}\cdot\text{m}^{1/2}$  at 1000 MPa yield strength), and matched the toughness goals for base metals ( $200 \text{ MPa}\cdot\text{m}^{1/2}$  at 1000 MPa yield strength).

Modification of the weld-pool deoxidation products is another way to reduce the number of inclusions. Aluminum is being evaluated as a deoxidizer and a possible replacement for the usual silicon deoxidizer. Preliminary tests indicate that sufficient strength can be obtained by using carbon instead of nitrogen as the primary strengthener, thus precluding the formation of AlN, which would weaken the weld.

#### Real-time radiology

The division hosted a workshop in April to develop a ranked list of national research priorities in real-time radiology. The twenty-three participants identified radiation transfer standards, source characterization standards, and image quantification as the top three needs. These priorities will guide NBS activities in standard development over the next five years.



## Thermomechanical Processing of Steels

Y.-W. Cheng, F. J. Fields, H. I. McHenry, D. Shepherd

Increasing the strength of a steel usually reduces its toughness. However, strength and toughness, especially the low-temperature toughness, can be increased simultaneously if the strength is realized through ferrite grain refinement. Further strength improvement with little sacrifice in toughness is obtained with bainitic structure and copper-precipitation strengthening. To achieve the optimum combination of strength and toughness of a steel through copper-precipitation strengthening, it is essential to select and control the time-temperature-deformation schedule used for hot rolling, the cooling after rolling, and the subsequent aging cycle. On the basis of fundamental metallurgical principles, a study of the thermomechanical process can produce the best rolling schedule.

### Simulator evaluation

A simulator has been built in the division's laboratory to study the thermomechanical processing of steels. The simulator, shown in figures 8 and 9, consists of a servohydraulic loading system, a vacuum system, an induction heater with gas cooling capacity, and a computer system for process control

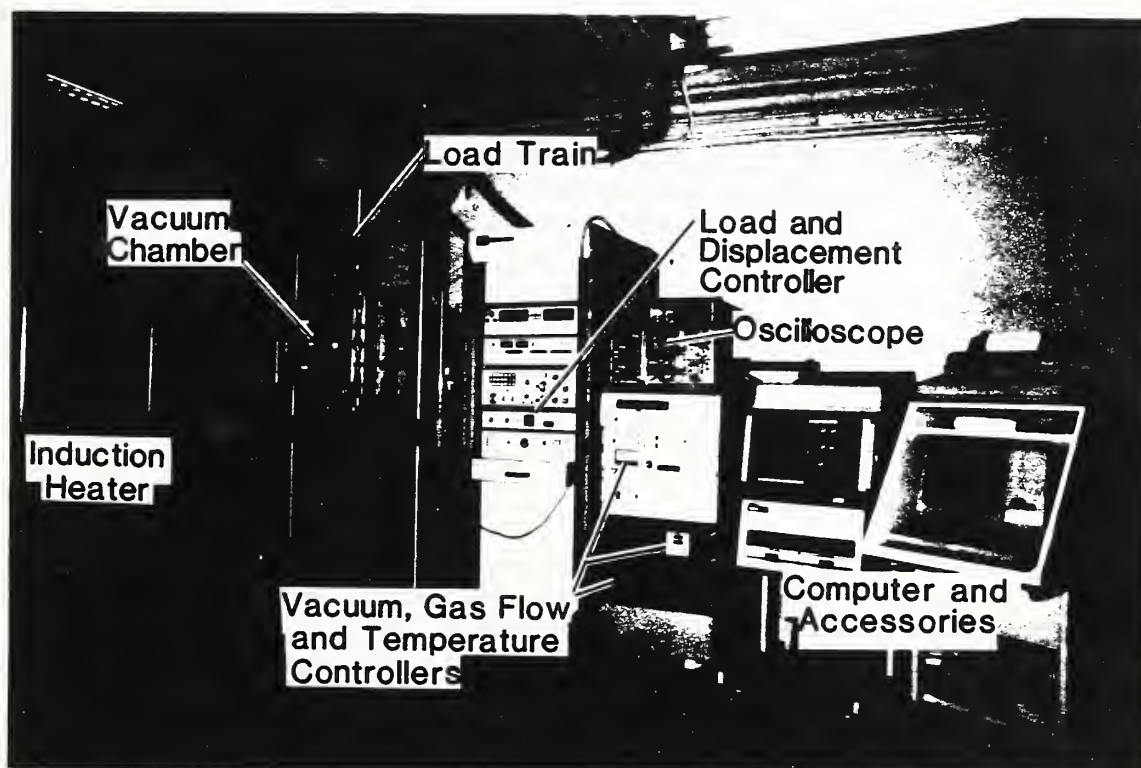


Figure 8. Hot-deformation simulator.

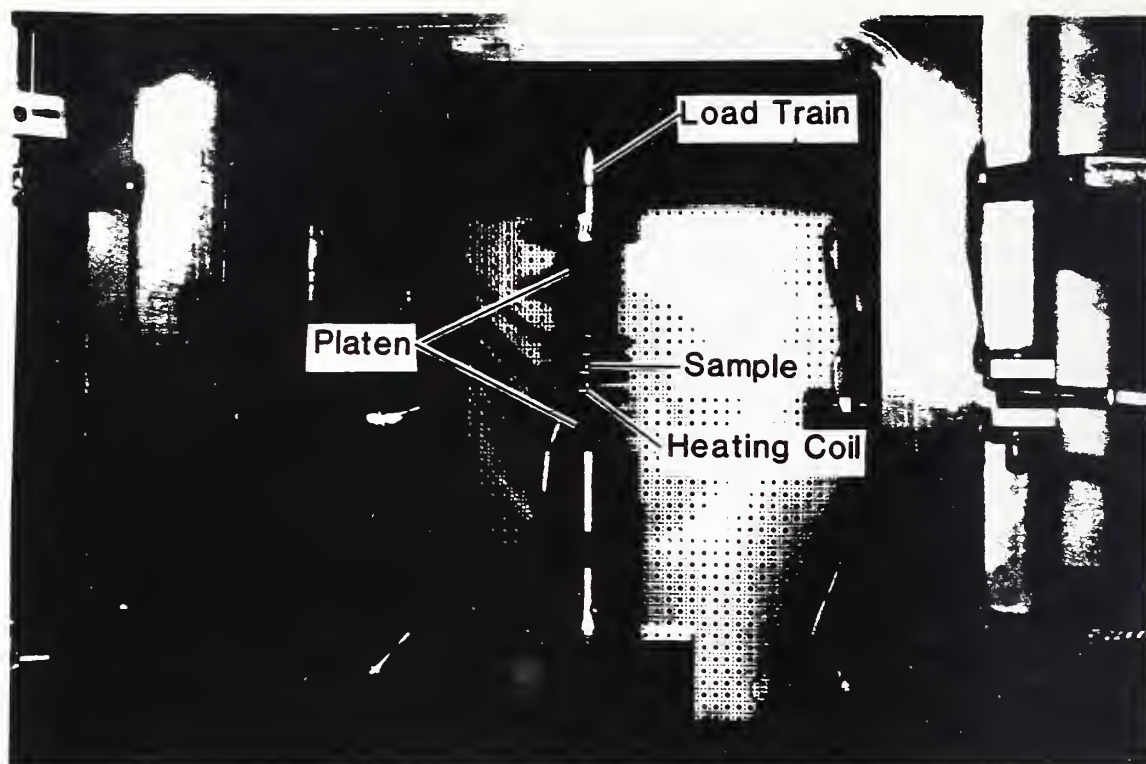


Figure 9. Interior of the vacuum chamber.

and data handling. It has the following features: 250-kN load capacity with a maximum actuator traveling speed of 50 cm/s; multistrike capability at different displacements and strain rates; a maximum heating rate of 150°C/s (for a cylindrical steel specimen 1.2 cm in diameter and 19.3 cm high); a maximum cooling rate of 25°C/s; and vacuum to  $1 \times 10^{-5}$  torr.

The simulator has been used to study the hot-deformation behavior of the A710 high-strength, low-alloy steel. Preliminary results indicate that under moderate straining, the steel does not undergo static recrystallization at 950°C.

#### Technology Implementation

The Department of Defense (DoD) plans to introduce thermomechanical processing into the U.S. steel industry. Steel companies participating in the DoD program\* will be given incentives to install the necessary equipment in the form of purchase commitments to purchase thermomechanically processed steel plates.

---

\*Defense Production Act Title III program: Accelerated Cooling Processing of DoD Steels.



We are assisting the U.S. Navy in the design of this program. Also, we are collecting technical data on the thermomechanical processing equipment used in Japan and the properties of the steel plates produced by this process.

#### Automated, Quantitative Microscopy

Thermomechanically processed steels will be characterized by two commercial, automated, television-microscopy systems. The systems have been programmed to measure the content, shape, and size distributions of nonmetallic inclusions in steel. Programs to measure grain shape and size distribution have also been developed.

Tests have demonstrated the accuracy of these programs for a resulfurized stainless steel containing a relatively high concentration of MnS inclusions. Inclusion content was measured about twelve hundred times to obtain a statistically appropriate distribution function (see figure 10). Neither of the conventionally assumed distribution functions (normal or log normal) was valid. At this time, a three-parameter Weibull distribution fits the data best. The correct distribution function is the basis for effective use of a smaller number of measurements or for the prediction of a rare event, such as the occurrence of a deleteriously large inclusion or inclusion agglomeration.

The two-dimensional data collected by this technique have been transformed by analysis into three-dimensional information. The algorithm worked correctly on an artificially constructed distribution of ellipsoidal inclusions. It has been successfully applied to sulfide inclusions in stainless steel. This approach is necessary to characterize the prior-austenite grain shape in steels rolled below the recrystallization temperature.



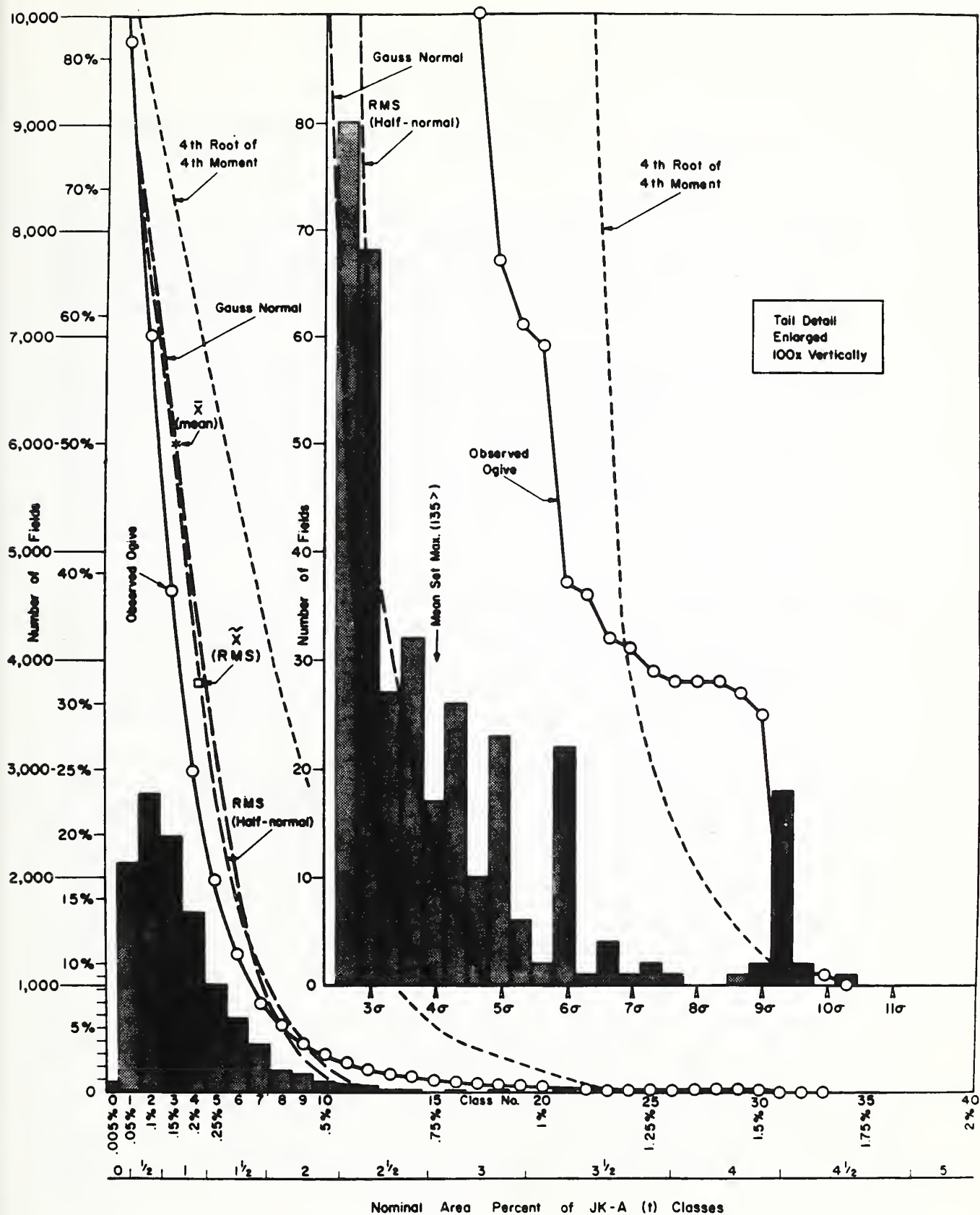


Figure 10. Distribution of inclusion concentration in resulfurized steel with various statistical measures or distributions for comparison.



# FRACTURE MECHANISMS and ANALYSIS

The goals of this task are to improve our understanding of the deformation and fracture behavior of materials and to apply this understanding to the assessment and improvement of the performance of materials. The research is distributed about equally among three groups of materials: metals and alloys, advanced composites, and cryogenic materials.

Mechanical deformation is composed of shear and dilation components. The elastic constants, which relate these deformations to stress, are physical properties; they, in turn, are related to various fundamental solid-state phenomena, including interatomic potentials, equations of state, and phonon spectra. Thermodynamics links elastic constants with specific heat, thermal expansivity, and the Debye temperature. Thus, the cornerstones of our research on deformation are measurements and modeling of elastic constants and related physical properties for the three groups of materials plus the new oxide superconductors.

Dislocation theory, which provides the theoretical basis for plastic deformation, has been helping us to understand fracture. Our work has emphasized two concepts: (1) dislocations can shield the crack tip from remote stresses and thereby toughen the material and (2) dislocation emission from the crack tip blunts the crack and forces crack growth to occur by ductile processes. Certain techniques used in these studies are proving to be powerful tools for modeling the fracture behavior of composite materials.

Composite materials have a wide range of mechanical properties that depend on the individual properties, amounts, and orientations of the constituents. Optimizing the formulation of a specific composite requires a model that relates the constitutive properties to the bulk performance. Our research has compared measurements and observations with the predictions of analytical models for a wide range of composite materials. Recent work has emphasized: (1) determining the residual stress state due to variations in the thermal expansivity of the components of a composite, (2) predicting the elastic properties of a composite on the basis of constitutive properties, and (3) studying the damage accumulation processes that precede fracture.

Characterization of mechanical performance is essential for making the best choice of structural materials for a given application. Over the years, we have evaluated many materials for various government agencies, and we have made many contributions to the development of standardized test procedures. This is particularly true in the area of cryogenic materials, which we have studied continuously for over thirty years. Our recent work has emphasized structural and insulating materials for superconducting magnets, copper for cryogenic magnets, indium for solder joints, and titanium for aerospace tankage.



## Representative Accomplishments

- Using scattered-plane-wave ensemble-average methods, we developed a new theoretical model to explain the elastic properties of porous ceramics. Predicting the porous-material elastic constants requires three ingredients: matrix elastic constants, pore volume fraction, and pore shape. For alumina, assuming disc-shape pores in the model yielded good agreement with measurements. Used inversely, the model yields the void-free-material elastic constants.
- The new high-critical-temperature metal-oxide superconductors,  $R_1Ba_2Cu_3O_{7-x}$  (R denotes a trivalent rare-earth cation), were studied by x-ray diffraction and ultrasonic waves. Superconductor properties depend strongly on the details of crystal structure and on the species of R atom, which lies at the unit-cell center. Against expectation, some of the superconductors, especially Ho-Ba-Cu-O, contain a magnetic phase together with the superconducting phase.
- By including the effect of applied stresses, which is neglected in traditional dislocation mechanics, the dislocation zone size was found to be inversely proportional to the net shear resistance of atomic motion. An expression for the activation energy required to nucleate a dislocation loop at crack tips in intrinsically brittle materials was derived. The results will be used to treat the transition from brittle-to-ductile behavior.
- As a part of the United States-Japan Cooperative Program for the Development of Cryogenic Mechanical Test Standards, a round-robin test program was conducted to evaluate the draft standards. Tensile and fracture tests of a Fe-13Cr-22Mn austenitic stainless steel at 4 K were conducted at seven laboratories in the United States and Japan. Drafts of proposed standard 4-K tensile and fracture toughness test procedures were written, reviewed, and revised. A matrix of tests was executed at four laboratories to provide data on test procedures.
- A new method has been used to study the cooling and heating in aluminum and steel under tensile and cyclic loading; it is based on the measurement of infrared emission from the surface of a loaded body. Test procedures have been developed to measure energy changes near the crack tip and the immediately surrounding area. The technique is also used to determine the position of the crack tip during cyclic loading.



## Physical Properties

H. M. Ledbetter, M. W. Austin, S. A. Kim, M. Lei\*

Physical properties studied by measurement, analysis, and modeling include sound velocities, internal friction, thermal expansivity, specific heat, magnetic susceptibility, volume (mass density), stacking-fault energy, phase transformation, internal strain (residual stress), and especially, elastic constants. We study many types of materials: metals and alloys, polymers, intermetallic compounds, ceramics, and composites, which include particle, fiber, and cloth reinforcement and both metallic and nonmetallic matrices. For many studies, the temperature ranges between 295 and 4 K. During the past year, we focused on three types of materials: austenitic steels, structural composites, and the new high-critical-temperature metal-oxide superconductors.

### **Austenitic steels**

We developed a new correlation between stacking-fault energy,  $\gamma$ , and the monocrystal elastic stiffnesses,  $C_{ij}$ . This correlation may permit us to publish several experimental studies by M. W. Austin: alloying effects of nickel, manganese, and carbon-plus-nitrogen in Fe-Cr-Ni alloys. If verified, the correlation provides many opportunities for further alloying studies.

We measured and modeled the effect of molybdenum on Fe-Cr-Ni-alloy volume. We ascribe the large volume change, unexplained by atomic volumes or elastic constants, to a 4d-electron bcc-paradigm metal located in a 3d-electron fcc crystal structure.

### **Composites**

Working with B. K. D. Gairola of the University of Stuttgart, we used an elastic-continuum model to predict the polycrystalline quasi-isotropic elastic constants of graphite. These calculations provide useful reference states for studying two materials: graphite fibers in composites; graphite nodules and flakes in cast iron.

With S. K. Datta of the University of Colorado, we published several studies that model composite-material interfaces, especially their effect on ultrasonic-wave velocity and attenuation. These results provide a basis for nondestructive study of interface properties.

---

\*Guest Worker from the Institute of Metal Research, Shenyang, China.

For a uniaxial glass-fiber-reinforced epoxy-matrix composite, we measured and modeled the torsional modulus and associated internal friction. Our model considered nonhomogeneous fiber distribution.

For  $\text{SiC}_p/\text{Al}$  composites, we measured and modeled elastic constants and internal friction. The model included particle-shape effects. Against expectation, internal friction increased with increased particle volume fraction.

We developed a model for the elastic constants of porous ceramics that applies also to porous superconductors (discussed below). Unlike all previous studies, our model considered nonspherical pores. For the test case, alumina, we obtained good agreement between observation and prediction if we assumed oblate-spheroidal (disc-shaped) pores (see figure 11). Both spherical and prolate-spheroidal pores fail to explain observation.

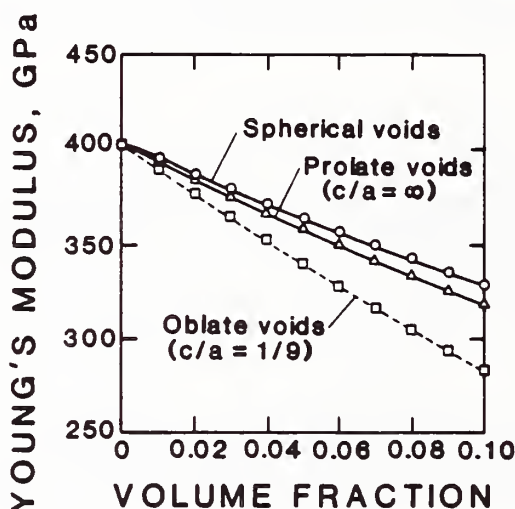


Figure 11. For Young's modulus versus pore volume fraction of alumina, this figure compares three sets of modeling results—for spheres, prolate-limit cylinders, and discs ( $c/a = 1/9$ )—with observation (dashed line).

### Superconductors

By ultrasonic methods, we measured the elastic constants of the new high-critical-temperature metal-oxide superconductors, especially  $\text{R}_1\text{Ba}_2\text{Cu}_3\text{O}_{7-x}$  (where R denotes a trivalent rare-earth cation), at temperatures between 295 and 4 K. Below and above the critical temperature, the elastic constants behaved irregularly. Some materials showed hysteresis. Figure 12 shows representative results.

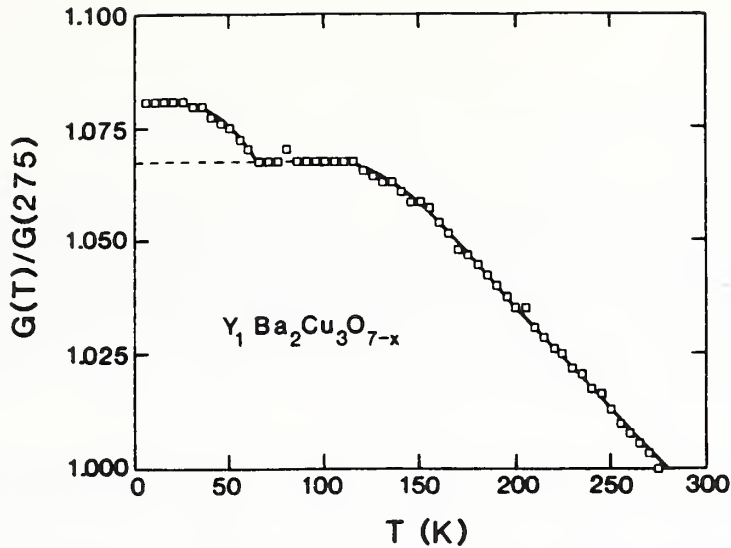


Figure 12. Relative shear modulus  $G = \rho v_s^2$  between 275 and 4 K. Above  $T_c$  (65 K), behavior is normal. Below  $T_c$ , contrary to expectation,  $G$  increases. Magnetic susceptibility,  $\chi$ , shows an abrupt decrease below 79 K, a  $d\chi/dT$  maximum between 60 and 65 K, and a zero in  $d^2\chi/dT^2$  at 62 K.

To complement the above study, we measured the low-temperature elastic constants of  $\text{BaTiO}_3$ , a building block for the superconductor. [To obtain  $\text{R}_1\text{Ba}_2\text{Cu}_3\text{O}_{7-x}$  crystal structure, stack three cubic  $\text{BaTiO}_3$  unit cells, remove one O atom at  $(0,0,1/2)$ , remove another at  $(1/2,0,0)$ , and allow relaxations.] The  $\text{BaTiO}_3$  results showed many surprises, which remain noninterpreted.

As mentioned above under Composites, we successfully applied our plane-wave-scattering ensemble-average models to the porous superconductors. This approach enabled us to determine the pore-free-superconductor elastic stiffness values, which are much softer than those for  $\text{BaTiO}_3$ .

#### Other materials

This year, other physical-property studies included beryllium, indium, a graphite-magnesium composite, a glass-epoxy composite, and cast iron.

## Fracture Physics

I.-H. Lin, R. M. Thomson\*

Research of the Fracture Physics Group is directed toward understanding (1) the toughness or brittleness of materials in terms of their fundamental properties and the interactions between cracks and dislocations and (2) the effects of external chemical environments on cracks in brittle materials.

### **Brittle-to-ductile fracture transition**

We have recently developed a theory of dislocation loop-nucleation under the influence of applied shear stresses. In it, we have shown that the activation energy required to nucleate a dislocation loop on a slip plane is strongly affected by the dislocation core size. For a given applied shear stress, the dislocation core size, which is inversely proportional to that stress, alters the critical dislocation loop size, and the activation energy is sensitive to the dislocation loop size.

This theory has been applied to the study of dislocation-loop emissions from sharp cracks. Work under way should establish the conditions under which dislocation-loop emissions occur throughout a zone surrounding the crack tip during the brittle-to-ductile transition in intrinsically brittle materials. Furthermore, with these ideas we hope to be able to understand and model the brittle-to-ductile transition temperature, because heat assists dislocation-loop emission processes at crack tips. We suggest that one important factor in the determination of the brittle-to-ductile transition temperature is the competition among the dislocation-loop emissions, dislocation propagation after nucleation, and shielding crack breakaway.

### **Model of composite ductile failure**

J. P. Hirth and I.-H. Lin have derived an expression for the thermodynamic force on line-force defects in which line forces describe the incompatibility strain field of a plate-like inclusion, precipitate, or composite laminate in a stressed matrix. We have begun to study the elastic interactions among inclusions, dislocations, and other defects. With this approach, we hope to achieve a better understanding of the ductility improvement in particle-reinforced aluminum composites, which we recently examined by a failure model of composites. In this model, we have assumed that voids nucleate at the particle-matrix interface and grow to a critical size at fracture. One adjustable parameter, the critical void size, was fit to results of uniaxial tensile tests. The model quantitatively predicts the tensile strains at fracture as a function of the SiC volume fraction. Preliminary comparisons of the model with observation look promising.

---

\*Institute Scientist, Institute for Materials Science and Engineering.

## Mixed-mode fracture

Knowledge of crack initiation and stable crack growth in combined mode-I and mode-III fracture is needed to understand ductile fracture in tough materials. The slope,  $M$ , in  $J_{III}$ - $J_I$  toughness space is a new parameter for characterizing mixed-mode fracture. To understand this failure, we have developed a stable-crack-growth model, in which the crack growth is both controlled by the applied mixed  $J$ -integrals and the injection of mixed superdislocations into the ductile materials from the crack tip. The emitted dislocations account for both the crack-tip plasticity and the crack-tip opening displacements. The value of  $M$  predicted by our simple model is 0.3 for stable crack growth, which is in good agreement with experimental results reported by Schroth et al.

## Dynamic crack velocity

We have developed a quasi-static crack model to predict two loci of the mode-I dynamic crack tip. At these loci, the crack tip induces corresponding maximum and zero difference strains, which are observed by strain gages located at some height above the crack plane. This calculation is applied to obtain instantaneous crack velocities in crack-arrest tests. The crack velocity calculated by this method is very accurate when it is less than about half the Rayleigh wave speed.

## Modeling the effects of a chemical environment

Generally, when modeling a crack-tip configuration, one relies on the Barenblatt approximation when the continuum is valid or on discrete treatments otherwise. When large external molecules enter a crack, they cannot penetrate it all the way to the tip. Then a combination of discrete and continuum views is desirable. When penetration of the external molecules is incomplete, some very interesting physical consequences occur in the structure of the tip owing to a wedging effect of the external molecules. A new theory has been developed for the observed activated crack growth, which incorporates the discrete effects at the crack tip with the long-range surface forces.



## Composite Mechanics

R. D. Kriz, P. R. Heyliger,\* H. M. Ledbetter, M. Lei,<sup>†</sup> J. C. Moulder

The emphases of our research are (1) the mechanics of fracture, (2) the mechanics of deformation, (3) nondestructive evaluation of laminated and fiber-reinforced composite materials, and (4) physical-property measurement and modeling. We develop models to predict the mechanical behavior of these materials, and whenever possible, we compare theory with experiment. Unlike conventional homogeneous isotropic materials, composite materials can be designed for specific applications by controlling their wide range of parameters, which include fiber volume fraction, interface properties, fiber orientation, laminate stacking sequence, and fiber-matrix elastic properties. We study how the design parameters relate to the mechanical and physical behaviors of the composites.

### Composite fracture mechanics

Fracture mechanics is not as well established for composites as it is for homogeneous isotropic materials. Therefore, our studies concentrate on the development of new methods to study the physical significance of different types of damage in laminated composites (i.e., ply cracks, interface cracks, edge stresses) that exist near bimaterial interfaces. We also measure the static strength and fatigue life of materials that are candidates for mechanical performance improvements.

**Mixed quarter-point elements in linear-elastic fracture mechanics.** The accuracy and efficiency of mixed finite elements in linear-elastic fracture mechanics problems were examined. Mixed elements possess displacement and stress degrees of freedom and generally have more rapid strain-energy convergence rates than displacement elements have. Conventional and quarter-point-element configurations were used to determine mode-I stress-intensity factors ( $K_I$ ) and total strain-energy values for several two-dimensional test geometries. The goals of this effort were to determine the effect of the quarter-point configuration on the behavior of the mixed element and also to determine the relative accuracy of different methods of computing  $K_I$ .

Three techniques were used to evaluate the stress-intensity factors: stiffness derivative, crack extension, and J-integral. The conventional and quarter-point mixed elements yield lower and upper bounds, respectively, of the strain-energy values for the geometries considered. The stress-intensity factors computed using conventional mixed elements were always less than those computed using mixed quarter-point elements; only when using the J-integral to compute  $K_I$  are the mixed quarter-point values more accurate.

---

\*NBS Postdoctoral Research Associate.

<sup>†</sup>Guest worker from the Institute of Metal Research, Shenyang, China.



In general, both configurations of the mixed elements gave very accurate (within 2 percent) values of  $K_I$  for very coarse meshes. The combination of these configurations enables rapid calculation of the bounds on the strain energy for a cracked body (see figure 13).

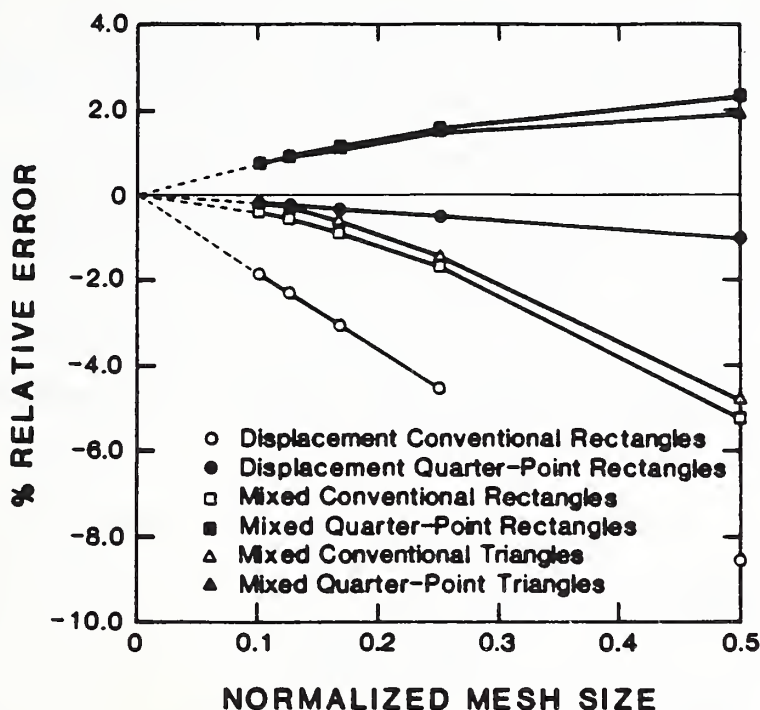


Figure 13. Strain-energy convergence for a double-edge-cracked panel for various finite-element configurations.

We also studied enriched mixed elements. Unlike the enriched displacement method, the enriched mixed method results in numerical singularities at crack-tip nodes. We are studying modifications of the present method to eliminate this problem.

**Analytical methods of calculating free-edge singularities.** We have successfully calculated the singularity at the bimaterial interface of a stress-free laminate by using Stroh's method. This singularity will be included in a generalized plane-strain enriched element. The total boundary value problem will be solved with the displacement method, where the coefficients of the singular terms are solved numerically along with the nodal displacements. Preliminary results indicate that these coefficients and their singular terms are extremely sensitive to the anisotropic elastic properties near the bimaterial interface. For isotropic materials, these coefficients are the well-known stress-intensity factors associated with the  $r^{-1/2}$  singular terms. If possible, the mixed enriched method will also be used to study this problem. Eventually, these methods will be extended to study the more complicated ply-crack problem.

**Edge stresses in woven composite laminates.** A finite-element model with generalized plane-strain elements was used to study the effect of weave geometry on the edge stresses. No singularities are included in this model; hence, stresses can be predicted only near the stress-free edge. Results of this study showed that the weave has a beneficial effect—it suppresses the initiation of damage at the stress-free edge. This prediction is supported by experimental observations: for some weave geometries, growth of damage that initiates inside the laminate is arrested near the free edge. For nonwoven laminates, the opposite is true: damage usually initiates at the stress-free edge and grows rapidly into the laminate. Future studies will include the interfacial stress-free-edge singularities.

**New composite material for thermal isolation straps.** In a study of advanced fiber-reinforced composites, we compared two thermal-isolation strap configurations, identical except for their fiber reinforcements: S2-glass and  $\text{Al}_2\text{O}_3$ . A popular cryogenic grade resin was used in both composites. Static and cyclic mechanical tests and thermal conductivity measurements indicated that the straps with  $\text{Al}_2\text{O}_3$  fibers were superior in performance. The fatigue test results for both materials are shown in figure 14. Other results of this study indicated that failure initiates in a region where the load is transferred by shear and compression.

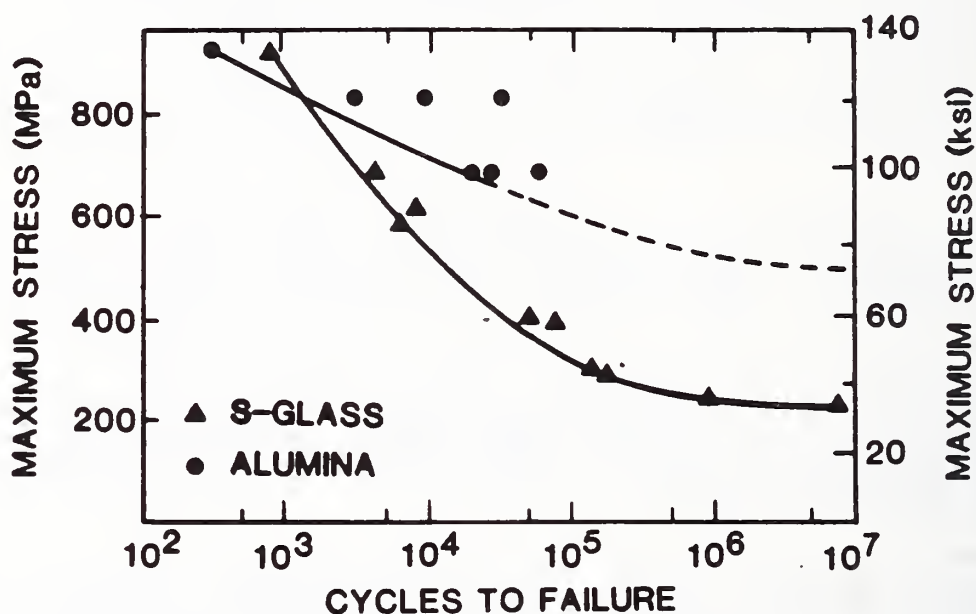


Figure 14. Strap fatigue test results at  $R = 0.05$  and 295 K.

#### Composite deformation mechanics

**Nonlinear response of rectangular beams from a theory of higher order shear deformation.** The Timoshenko theory has been used almost exclusively in the study of the static and dynamic behavior of shear deformable rectangular beams. The primary deficiency of the Timoshenko theory is the presence of the shear coefficient  $k$ , which is introduced to account for the contradic-

tory shear distribution over the cross section of the beam. The search for the best shear coefficient has been described as a "small research industry." In the literature, typical values for beams of rectangular cross section range from 0.822 to 0.870.

Higher order beam theory was used to study moderately large deflections and moderately large amplitude vibrations of rectangular beams with various boundary conditions. It allows for shear deformation and correctly accounts for the stress-free boundary conditions on the upper and lower surfaces of the beam. This higher order theory results in a model that is more theoretically sound than the Timoshenko theory because the need for a shear coefficient is eliminated. The resulting finite element equations are based on the minimum continuity requirements of the higher order theory. They do not require the reduced integration that is essential in the use of Timoshenko beam elements to eliminate numerical difficulties (locking), which can occur when the beam is thin.

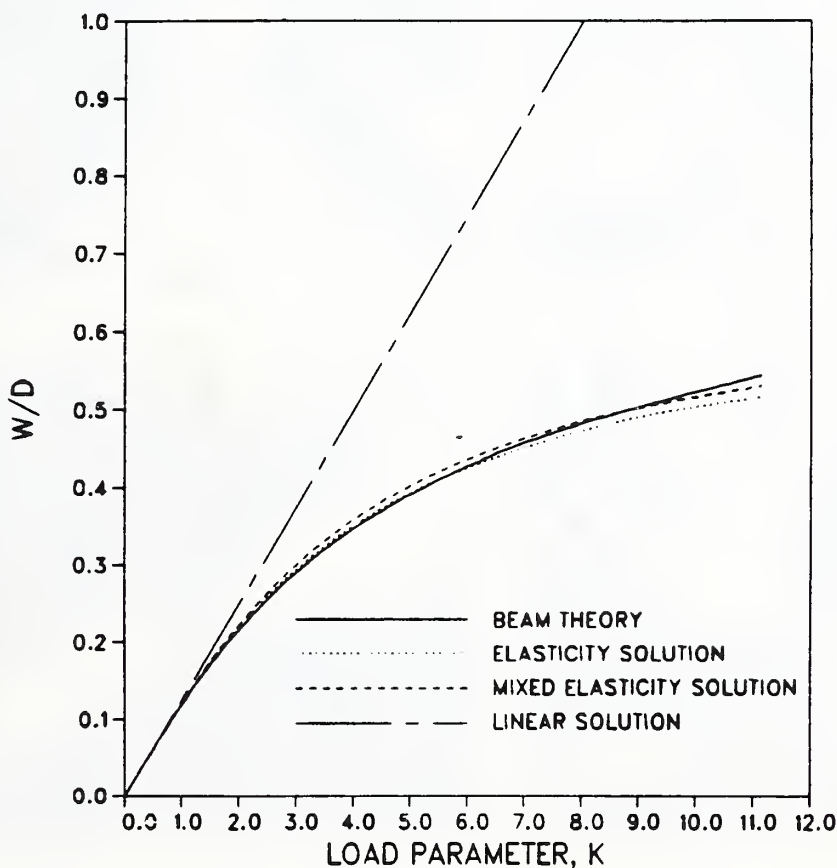


Figure 15. Nondimensional tip displacement of a uniformly loaded cantilever beam.

Solutions were obtained for static and dynamic response problems. The results obtained using the higher order theory are in excellent agreement with existing solutions for isotropic beams (see figure 15). The theory may be extended to analyze composite beam components consisting of layered isotropic materials.

### **Mechanics of nondestructive evaluation for composites**

Our nondestructive evaluation studies concentrate on (1) measuring and mapping the mechanical deformation near damage in a composite laminate by optical methods and (2) developing a numerical model of a capacitive-array sensor to monitor cracks in conductors (graphite fibers) and dielectrics (epoxy matrix).

**Determination of whole-field strain in a composite panel using coherent optical processing.** A newly devised video-optical experimental technique enables automated determination of the in-plane, plane stress components of the infinitesimal deformation tensor at discrete locations over an area of interest in a loaded specimen. It was used to evaluate a square area enclosing the central crack in a G10-CR woven glass-epoxy panel loaded in tension. A finite-element analysis modeled the strain tensor field surrounding the central crack. The experimental and the finite-element-analysis results were compared along the plane of the crack, along a plane above and parallel to the plane of the crack, and finally, along a plane perpendicular to the plane of the crack close to the singularity at the crack tip. The experimental and finite-element-model results are qualitatively equivalent and show the localized effect of high strains close to the crack tip. This localized effect in the composite panel is illustrated in figure 16, where the results are compared with a similar center-cracked aluminum panel.

**Numerical modeling of capacitive-array sensors.** A numerical model was developed for a capacitive-array sensor, which can be used in detecting flaws in dielectric and metallic plates. The simulated probe response was computed from the change in admittance (figure 17a), which is calculated from a line integral that is a function of the scalar potential and its normal derivative with respect to the specimen surface. The electrostatic potentials (figure 17b) and their gradients were computed from a two-dimensional finite-element model.

Parametric studies were performed on homogenous, isotropic specimens to determine the relative effects of flaw size, specimen dielectric constant, and probe lift-off distance. In general, the responses to flaws in dielectric specimens saturate for much smaller flaw sizes than do similar curves in conducting specimens.

Future applications of this model will include the detection of subsurface graphite fiber (conductor) breaks in an epoxy (dielectric) base for the nondestructive evaluation of graphite-epoxy composites. Because the electrostatic field penetrates the dielectric medium, subsurface flaws in the composite resulting from a material or field discontinuity may be readily detected using the present model.



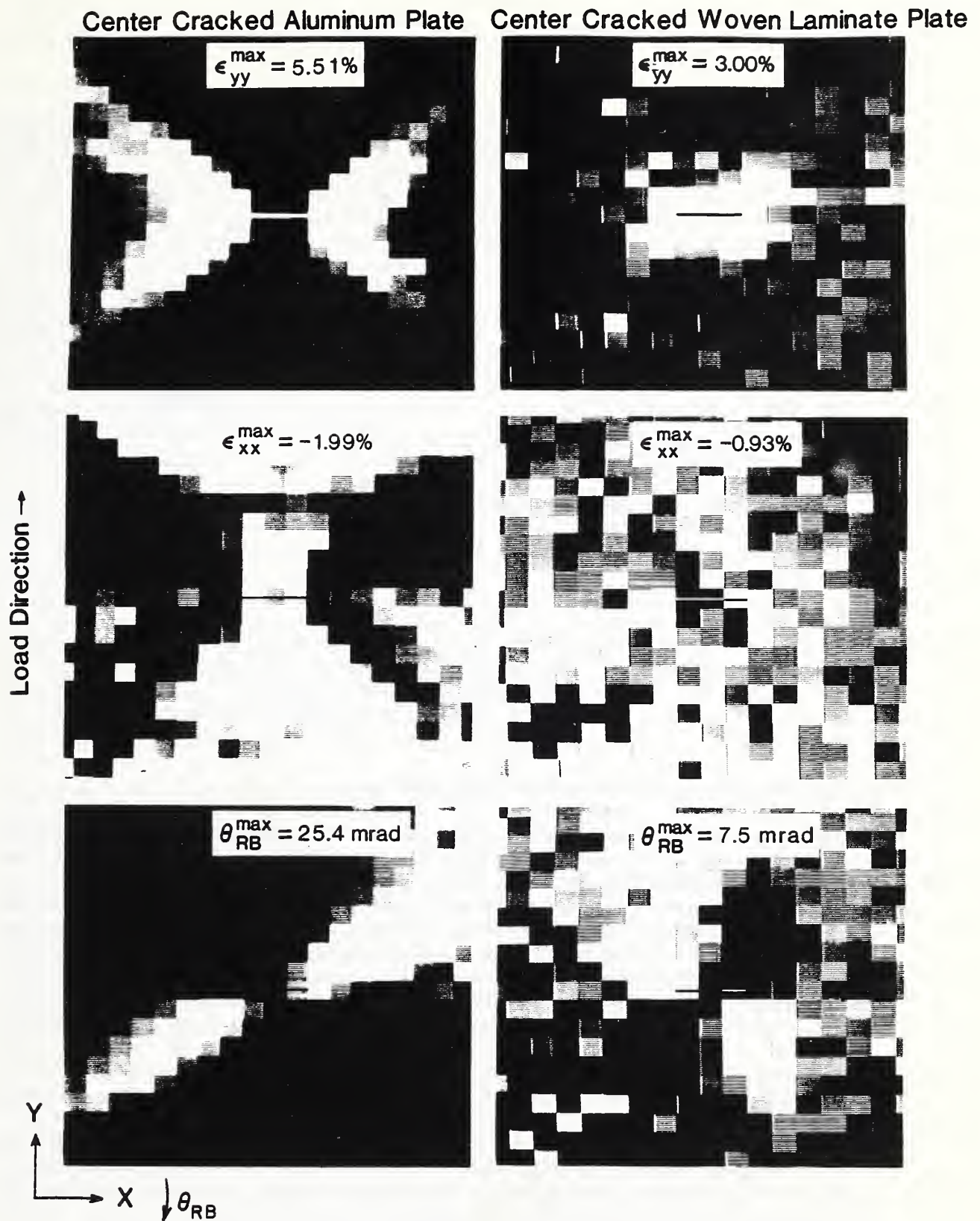


Figure 16. Comparison of strain fields for (a) center-cracked aluminum plate and (b) center-cracked woven laminate plate. The light areas indicate regions of high strain.

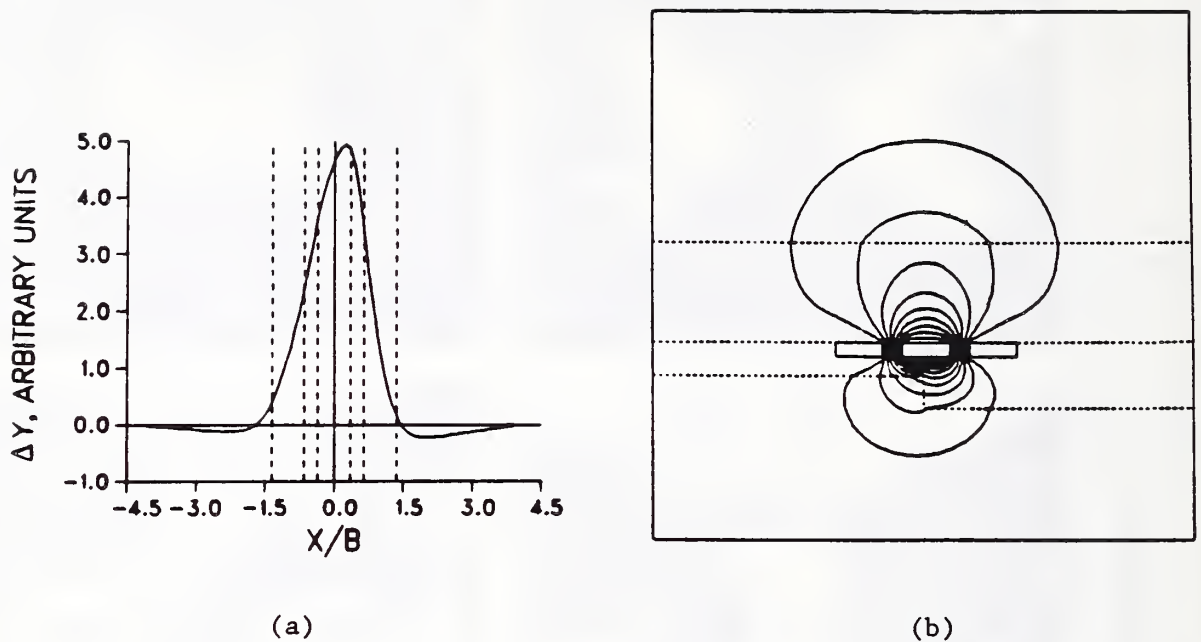


Figure 17. Response of the capacitive array probe for a flaw in a dielectric specimen.  
 (a) change in admittance;  
 (b) potential for step in specimen.

#### Physical-property measurement and modeling

We focus on several composite-material physical properties: sound velocities, mass density, elastic constants, internal friction, thermal expansivity, and specific heat. These properties depend on constituent properties (both occluded phase and matrix) and occluded-phase geometry. For the occlusion, phase geometry includes volume fraction, shape, orientation, size, and distribution nonhomogeneity. We developed theoretical models and accompanying computer programs that apply to a wide variety of composites: particle, fiber, cloth, laminated reinforcements; plastic or metal matrices; rod-shaped or disc-shaped particles; composites with voids.

**Modeling.** We considered the phase velocity and attenuation of plane elastic waves in a particle-reinforced composite medium. Our study considered effective-plane-wave propagation, both longitudinal and shear, through a medium containing a random distribution of spherical inclusions. We assumed that the particles and matrix are separated by a thin layer of elastic material with different properties. For some systems, we predict measurable effects for the thin layers. Especially, we considered Pb/epoxy and SiC/Al, laboratory and practical materials, respectively.

Using theoretical models, we considered the elastic constants of ceramics containing pores. As an example, we considered alumina. However, the



approach applies to all ceramics. As a point of departure, we considered spherical pores. For all the usual elastic constants—Young's modulus, shear modulus, bulk modulus, Poisson's ratio—we derived relationships for both the forward and inverse cases: predicting the porous ceramic properties and estimating the pore-free ceramic properties. Following a suggestion by Hasselman and Fulrath that sintering or hot pressing can produce cylindrical pores, we derived a relationship for the elastic constants of a distribution of randomly oriented long cylinders ( $c/a = \infty$ , the prolate-spheroid limit). This model predicts elastic constants lower than those for spherical pores, but well above observation. We obtained agreement with observation by assuming the pores are oblate spheroids. For alumina, the necessary aspect ratio equals one-ninth. Using this oblate-spheroid pore-shape model, we calculated all the elastic constants versus pore volume fraction for alumina. Besides pore aspect ratio, the model requires only the pore-free alumina elastic constants. It contains no adjustable parameters.

**Measurement and modeling.** Using dynamic methods, we measured the Young's and shear moduli of aluminum-matrix particle-reinforced composites containing up to 55 volume percent SiC particles. Using a scattered-plane-wave ensemble-average model, we calculated four elastic constants: Young's, shear, and bulk moduli and Poisson's ratio. The model uses four kinds of information: matrix elastic constants, particle elastic constants, particle volume fraction, and particle shape. Between measurement and calculation, we found good agreement. As expected, the elastic stiffnesses fall well below a rule-of-mixture prediction; the Poisson's ratio falls above. Also, we measured the Young's-modulus-mode internal friction, which, contrary to expectation, increases with increasing particle content.

By a kilohertz-frequency resonance method, we determined the torsion modulus and internal friction of a uniaxially fiber-reinforced composite. The composite comprised glass fibers in an epoxy-resin matrix. We studied three fiber contents: 0, 41, and 49 volume percent. The internal friction failed to fit a classical free-damped-oscillator model where one assumes a linear rule of mixture for three quantities: oscillator mass, force constant, and mechanical-resistance constant. The torsion modulus fit approximately a plane-wave-scattering ensemble-average model. The microstructure showed strong fiber-distribution nonhomogeneity. Considering this nonhomogeneity yielded better agreement between model and observation. Thus, torsion-modulus measurements provide a method to detect and quantify fiber-distribution nonhomogeneity.

**Analysis.** We considered the directional variation of elastic constants of a uniaxial graphite-fiber-reinforced magnesium-matrix composite. Unidirectional graphite-magnesium composites show high elastic anisotropy and unusual geometrical features in their elastic-property polar diagrams (see figure 18). From the five-component transverse-isotropic elastic-stiffness tensor we computed and graphed representation surfaces for Young's modulus, torsional modulus, linear compressibility, and Poisson's ratios. On the basis of Christoffel's equations, we described some unusual elastic-wave-surface topological features. For graphite-magnesium, we predicted some

new results: a shear-wave velocity that exceeds a longitudinal-wave velocity in the plane transverse to the fiber, a wave that changes polarization from longitudinal to transverse as the propagation direction sweeps from the fiber axis to the perpendicular axis. Our study emphasizes the importance of obtaining the complete elastic-stiffness tensor. We considered examples of errors resulting from popular elastic-constant approximations.

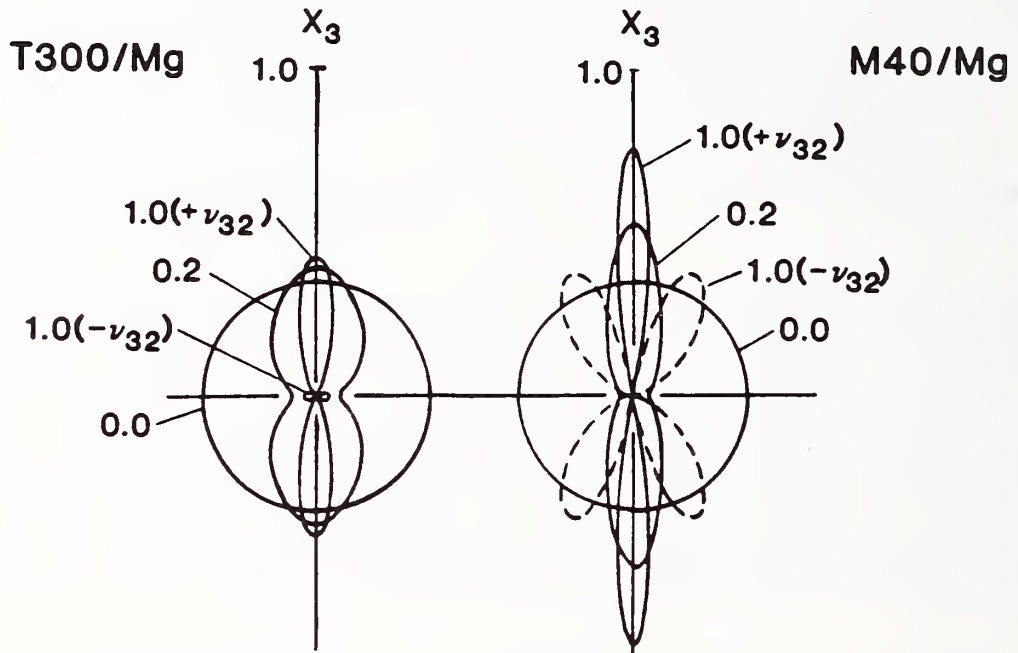


Figure 18. Polar diagram of Poisson's ratio  $\nu_{32}$  for various fiber volume fractions.

## Cryogenic Materials

R. P. Reed, L. M. Delgado, J. K. Han,\* T. Ogata,† P. T. Purtscher,  
N. J. Simon, R. L. Tobler, R. P. Walsh

### Adiabatic heating calculations

Internal specimen heating effects during low-temperature tests of mechanical properties have been questioned for a long time. The very low specific heat and thermal conductivity of metals at low temperatures lead one to anticipate near-adiabatic conditions. Discontinuous yielding, a phenomenon in which very high strain rates are experienced in local regions (similar to Lüders band regions in steel at ambient temperatures), complicates the question, and the answer is prerequisite to the establishment of test standards.

Tensile stress-strain curves at differing strain rates are shown in figure 19. At the lower two strain rates, discontinuous yielding is prominent. At the highest strain rate, discontinuous yielding is less evident, the curves have an erratic appearance, and reduction of ultimate strength is apparent. Clearly, the nature of the deformation process has changed. The onset of discontinuous yielding is dependent on both alloy and strain rate.

The temperature measurements of thermocouples attached to the central portion of the specimens surfaces are also included. Notice the change from thermal spikes at lower strain rates to thermal waves at the highest strain rate. The thermal spikes are associated with individual discontinuous yielding events. The thermal waves, which gradually build up to temperatures as high as 96 K, are associated with the lack of discrete discontinuous yields and with the wavy nature of the stress-strain curves. Reduction of tensile strength is associated with this thermal transition.

Our calculations have been completed. They estimate the work put into a specimen during deformation, the stored energy in terms of dislocations and dislocation interactions, and the dissipated heat. These contributions, equated in terms of a specimen heat balance, indicated that the reduction of strength at high strain rates is associated with specimen warming, which is caused by the transition from nucleate to film-boiling heat transfer on the specimen surface.

---

\*Guest worker from Korea Advanced Institute of Science and Technology, Seoul, Korea.

†Guest worker from the National Research Institute for Metals, Ibaraki, Japan.

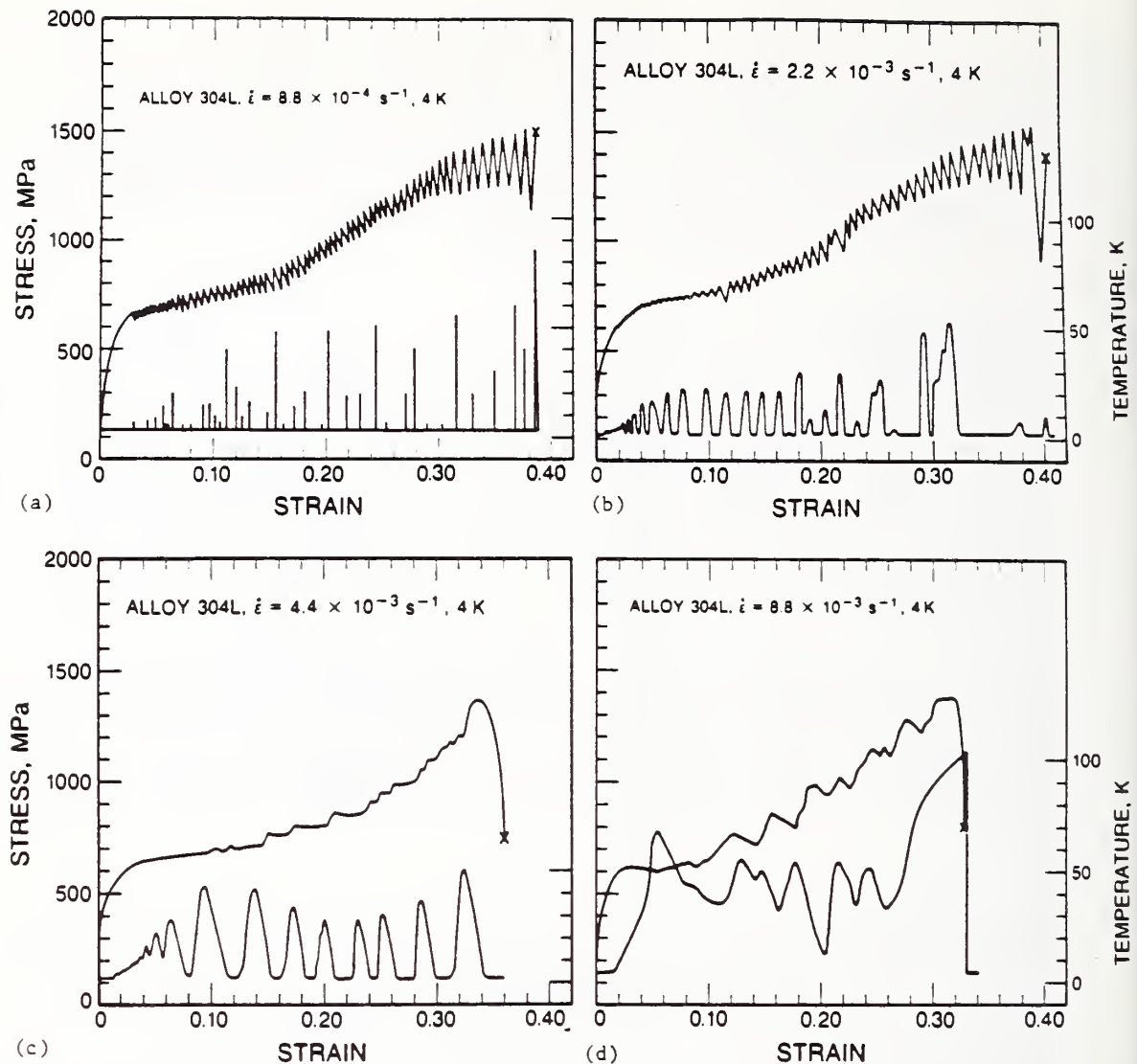


Figure 19. Stress-strain curves and specimen surface temperatures at various strain rates for alloy 304L.

#### Effects of loading rate during tensile tests at 4 K

We investigated the effects of loading rate on the tensile properties of AISI 304L, 310, and 316LN steels through load-control tensile tests at 4 K. Usually, the tensile properties of structural materials at 4 K are obtained from displacement-control tensile tests in which discontinuous deformation occurs accompanied by load drops and temperature rises. Discontinuous deformation is different in load-control tensile tests: (a) no load drop occurs during the deformation because the amount of displacement is not limited by the testing machine and (b) the measured ultimate strength is



lower. This deformation behavior affects the mechanical properties of structural materials at low temperatures under load-controlled deformation. From load-control tensile tests in which the loading rates were varied from 0.5 N/s to 5 kN/s, we obtained the following results:

1. Ultimate tensile strength decreased with increased loading rate, reflecting increased specimen heating; at 5 kN/s it was 65 percent of the ultimate strength obtained in displacement-control tests. Thus, a freely deforming material at low temperatures will fail at a much lower stress than one whose deformation is controlled.
2. AISI 310 specimens deformed 2 percent at just 3 percent above the yield strength when 500 N/s was applied. At 5 N/s, AISI 310 specimens deformed significantly—15 mm—near 40 percent strain; rapid deformation occurred along the entire specimen length. Average deformation velocities were 26 mm/s ( $7.5 \times 10^{-1} \text{ s}^{-1}$ ). This deformation was accompanied by local specimen heating, which stopped when a balance of the local strength and work hardening was reached. Subsequent discontinuous deformations occurred in other areas of the specimen where there had been less local strain hardening.
3. AISI 304L specimen elongation was not affected by either the loading rate or the control mode. This is due to its lower yield strength and its high work hardening accompanied by martensitic transformation. The transformation caused interrupted and unstable deformation.

#### Effects of specimen variations on J-integral test results

We cooperated with researchers from the National Research Institute for Metals in Ibaraki and Tohoku University in a study of the J-integral test at 4 K, in support of the development of a standard test procedure.

The tests used a computer-controlled unloading-compliance technique, a single-specimen method that is especially useful at 4 K, on compact specimens of AISI 316LN alloy. The test variables were:

- specimen size, 12.5, 25, and 38 mm thick (0.5TCT, 1TCT, and 1.5TCT)
- fatigue precracking temperature, 293, 77, and 4 K at a stress-intensity factor of about  $24 \text{ MPa} \cdot \text{m}^{1/2}$
- plain and side-grooved specimens

The effects of the test variables are shown in figure 20. Toughness decreased with increasing specimen thickness, at least from 25 to 38 mm. The toughness of the side-grooved specimens was less than that of plain specimens, but the effect was small—less than 10 percent in the largest specimen. The effects of specimen thickness and side-grooving are related to the constraint exerted at the crack tip. Fatigue precracking temperature had a significant effect on the size of the plastic zone of the specimen, but had no measurable effect on the fracture toughness at 4 K.

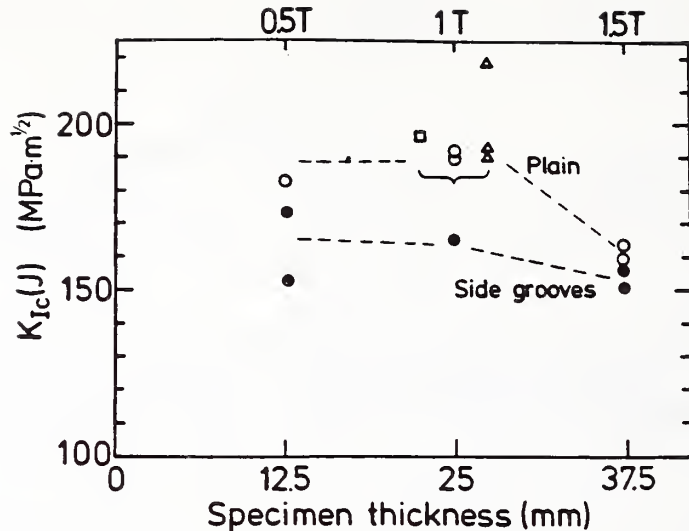


Figure 20.  $K_{IC}(J)$  estimates at 4 K as a function of thickness for proportionally sized specimens ( $W/B = 2$ ), showing the effects of side grooves. Symbols indicate fatigue precracking temperatures:  $\Delta$  - 293 K, o or  $\bullet$  - 77 K, and  $\square$  - 4 K. Open symbols indicate plain specimens; closed symbols, specimens with side grooves.

#### Copper processing for cryogenic performance

In the annealed condition, copper is usually not strong enough for use as the stabilizing element for low-temperature superconductors or as a high-field magnet conductor. It must be strengthened or reinforced. Two conventional ways to strengthen copper are cold working and reduction of grain size. Yet quantitative low-temperature property data on the effects of these metallurgical variables are not available. Therefore, we studied the effects of grain size variation and cold rolling on the tensile properties and electrical resistivity of copper at 4, 76, and 295 K.

We found that cold rolling dramatically increases yield strength, ultimate strength, and electrical resistivity; it reduces elongation, but does not affect reduction of area. Cold rolling to 10 percent reduction in thickness increases the yield strength by a factor of about 8 at all low temperatures; subsequent rolling to 60 percent increases the yield strength by a factor of only about 1.5. Tensile strengths are related to  $d^{-1/2}$ , where  $d$  is the grain size, following the Hall-Petch relationship. This dependence increases at low temperatures. Grain size has little effect on resistivity. On the basis of optimal strength and minimal resistivity, a modest amount of cold rolling (about 10 percent) produces the best ratio of strength to resistivity at low temperatures.



## United States-Japan program for the development of test standards

A United States-Japan cooperative program is developing tensile and fracture toughness testing standards for austenitic stainless steels (superconducting machinery construction materials) at 4 K. Sponsors of the program are the U.S. Department of Energy and the Japan Atomic Energy Research Institute (JAERI). Contributing organizations include NBS and four Japanese laboratories: JAERI, Tohoku University, Kobe Steel, and the National Research Institute for Metals.

During the past year, cryogenic materials scientists were interviewed at government, industrial, and academic institutions in Japan. Workshops were held in Sendai, Tokai-mura, and Reno. The first round-robin tensile and fracture tests of a Fe-13Cr-22Mn austenitic stainless steel at 4 K were conducted at seven laboratories in the United States and Japan. Five drafts of a proposed standard 4-K tensile test procedure were written and submitted to the workshops for review. Five drafts of a proposed 4-K fracture standard were also reviewed, and a matrix of tests was executed at four laboratories to answer questions about test procedures. Six joint research papers have been accepted for publication. Following final revisions, the test standards will also be submitted to ASTM for consideration as an ASTM standard.

## Material properties handbook

The Materials Handbook for Fusion Energy Systems (MHFES) is being developed to provide an authoritative common source of material properties for the fusion energy community to use in concept evaluation, design, safety analysis, and performance prediction and verification of fusion energy systems. This single source for properties is essential to ensure a common basis for comparing the eventual performance and economics of the various fusion systems currently under study, in operation, or under construction.

We are continuing to work on handbook pages for the MHFES covering low-temperature properties of structural alloys for the superconducting magnets used for plasma confinement in fusion energy devices. Three nitrogen-strengthened austenitic stainless steels that are the most promising near-term candidates for structural use in superconducting magnets were chosen for initial coverage. Initial work for preparation of handbook pages on aluminum alloys has been completed. Current work involves a review of properties of several high-purity coppers and copper alloys: CDA 101, 102, 104, 105, 107, 155, and 170 through 175.

## Material Performance

R. J. Fields, C. H. Brady, B. W. Christ, R. deWit, G. E. Hicho, Y. Huang,\*  
T. R. Shives, L. C. Smith

### Structure and properties of a high-strength, low-alloy steel

Our efforts to understand the relationship between the properties and structure of alloy A710 are continuing. To be acceptable for naval applications, the A710 steel must meet the bulge-test specification requirements. This test is usually performed after all the mechanical tests, and occasionally the plate material fails the bulge test. Plates of A710 steel that had passed or failed the bulge test were subjected to strain-hardening experiments; their texture was studied by means of pole figures. The 22 steel plates were statistically analyzed: each element and selected pairs of elements were compared with each other, and the overall composition was compared with that of the A710 steel that passed or failed the bulge test. Statistical results indicated that a correlation exists between the chemical composition of the steel and its ability to pass the bulge test, enabling naval engineers to predict success or failure prior to the extensive mechanical tests.

### Infrared method of studying crack growth

A new thermographic method has been developed that is based on the measurement of infrared emissions from the surface of a loaded body. It measures the thermoelastic cooling phenomenon during the tensile process and cooling and heating during cyclic loading. This method has been recently used to determine crack tip position during cyclic loading. It has improved the accuracy of crack-growth measurements, which are the basis for evaluating the fracture toughness of aluminum and steel plates used in tank cars.

### Compression tests of copper-Inconel laminates

With the successful explosive bonding of C10700 copper layers in between two layers of Inconel 718 and the promising progress in numerical modeling of the composite material, a program of composite material characterization and model verification was initiated.

The program consisted of a series of face compression tests, in uniform axial compression, at room temperature. The procedures of this program were:

1. Examine the single-cycle mechanical characteristics. Establish the 0.2-percent yield point. Explore well into the plastic range.

---

\*Guest Worker from the Institute of Metal Research, Shenyang, China.

2. Examine the low- and moderate-cycle behavior (at 10 and 3000 cycles) at loads approaching 75 percent of yield.

Tests were performed on the 53-MN ( $12 \times 10^6$ -lbf) NBS universal testing machine. Support equipment included displacement gages, bridge amplifiers, a digital oscilloscope, a wide-band FM magnetic tape recorder, and a micro-computer.

Test specimens were 18, 20, or 23 cm (7, 8, or 9 in) in diameter; their thickness varied from 2 to 3.5 cm (0.8 to 1.4 in). They were supplied by Princeton Plasma Physics Laboratory.

The general experimental procedure consisted of a number of static and two cyclic tests in each series. In step 1, the stress-strain curve for a given configuration was established by gradual loading (about 7 MPa/s, 1 ksi/s) while monitoring both diametric and axial displacements in real time. The tests were usually carried to an axial displacement of 0.38 mm (0.015 in), well into the plastic range. From these test results, the 0.2-percent yield point was established. For the 20-cm (8-in) diameter specimens, this occurred at about 20 MN ( $4 \times 10^6$  lbf) or 550 MPa (80 ksi).

In step 2, the load level representative of 75 percent of yield was established from the results of step 1 for two new specimens of the same type. The specimens were then cycled at 0.03 Hz for three thousand times at this load. For the 20-cm-diameter specimens, this was a load range from 2 to 10 MN (0.5 to  $3 \times 10^6$  lbf). For the second specimen in each series, the load range was increased in periodic steps until it was beyond the yield point. In these cases, the displacement gages revealed a significant amount of cyclic creep at the higher loads. Nevertheless, these specimens sustained loads well above the yield strength (69 to 370 MPa, 10 to 53 ksi) and tensile strength (220 to 455 MPa, 32 to 66 ksi) of copper.

#### **Failure examinations for the Potomac Electric Power Company**

During the past year, we have presented to the Potomac Electric Power Company (PEPCO) twenty-three reports on failures that occurred in their power generating equipment. Our failure analyses were diverse: from the quality of welding in two water-wall tubes that were joint to whether an existing crack followed an electrical resistance weld. Some of our failure analyses had to be done very quickly to keep the nonoperating time of the power generating unit to a minimum. In addition to determining the causes of these failures, we have assisted PEPCO as consultants on replacement materials for those that failed.

#### **Mechanical Failures Prevention Group**

At the request of the Naval Air Test Center (NATC), the Mechanical Failures Prevention Group (MFPG) held its 41st meeting in October 1986 at NATC in Patuxent River, Maryland. The subject of the three-day symposium was Detection, Diagnosis, and Prognosis of Rotating Machinery to Improve Reliability, Maintainability, and Readiness through the Application of New and Innovative

Techniques. About 235 people attended. The meeting was sponsored by NBS and the Office of Naval Research in cooperation with the American Helicopter Society.

The 42nd meeting of the MFPG was held in September 1987 at NBS-Gaithersburg. The theme of the meeting, Technology Innovation - Key to International Competitiveness, was intended primarily for the small business community. About 95 people attended. The three-day meeting was cosponsored by NBS and the Office of Naval Research. Cooperating organizations included the Small Business Administration, Battelle Pacific Northwest, and the University of Maryland.

**OUTPUTS  
and  
INTERACTIONS**





### SELECTED RECENT PUBLICATIONS\*

Cardenas-Garcia, J. F.; Moulder, J. C.; Kriz, R. D. Video optical determination of a whole-field strain in composite panel. Optical Methods in Composites. Bethel, Connecticut: Soc. Exper. Mech.; 1986 October. 48-57.

Cheng, Y.-W. Fatigue crack growth analysis under sea-wave loading. Int. J. Fatigue; accepted.

Cheng, Y.-W.; Broz, J. J. Cycle-Counting Methods for Fatigue Analysis with Random Load-Time Histories: A Fortran User's Guide. Nat. Bur. Stand. (U.S.) NBSIR 86-3055; 1986 August. 52 pp.

Clark, A. V.; Fukuoka, H.; Mitracović, D. V.; Moulder, J. C. Ultrasonic characterization of residual stress and texture in cast steel railroad wheels. Thompson, D. O.; Chimenti, D. E., eds. Review of Progress in Quantitative Nondestructive Evaluation, vol. 6B. New York: Plenum, 1987; 1567-1575.

Clark, A. V.; Govada, A.; Thompson, R. B.; Smith, G. F.; Blessing, G. V.; DelSanto, P. P.; Mignogna, R. B. The use of ultrasonics for texture monitoring in aluminum alloys. Thompson, D. O.; Chimenti, D. E., eds. Review of Progress in Quantitative Nondestructive Evaluation, vol. 6B. New York: Plenum; 1987. 1515-1524.

Clark, A. V.; Moulder, J. C.; DelSanto, P. P.; Mignogna, R. B. A comparison of several ultrasonic techniques for absolute stress determination in the presence of texture. Achenbach, J. D.; Rajapakse, Y., eds. Proceedings, Symposium on Solid Mechanics Research for Qualitative NDE. Dordrecht, The Netherlands: Martinus Nijhoff; 1987. 345-360.

Clark, A. V.; Moulder, J. C.; Mignogna, R. B.; DelSanto, P. P. Ultrasonic determination of absolute stresses in aluminum and steel alloys. Proceedings, International Conference on Residual Stress; accepted.

Clark, A. V.; Moulder, J. C.; Mitracović, D. V.; Fukuoka, H. Ultrasonic characterization of residual stress and texture in a heat-treated steel railroad wheel. Mater. Eval.; accepted.

Clark, A. V.; Read, D. T. Ductile Tearing Stability Analysis of a Ship Structure Containing a Crack Arrestor Strake. Nat. Bur. Stand. (U.S.) NBSIR 85-3038; 1986. 48 pp.

Danko, B. A.; Low, S. R., III; deWit, R.; Fields, R. J. Wide plate crack arrest tests: instrumentation for dynamic strain measurements. Shives, T. R., ed. Use of New Technology to Improve Mechanical Readiness, Reliability, and Maintainability. London: Cambridge University Press; 1987; 178-192.

---

\*Papers that were published or accepted for publication by NBS Editorial Review Boards during fiscal year 1987.

Datta, S. K.; Ledbetter, H. M. Ultrasonic-velocity studies in metal-matrix composites: measurements and modeling. San Antonio, Texas: Nondestructive Testing Information Analysis Center; Santa Barbara, California: Metal Matrix Composites Information Analysis Center; Columbus, Ohio: Metals and Ceramics Information Center; 1986. 41-62.

Datta, S. K.; Ledbetter, H. M.; Shindo, Y.; Shah, S. H. Interface effects on attenuation and phase velocity in metal-matrix composites. Thompson, D. O.; Chimenti, D. E., eds. Review of Progress in Quantitative Nondestructive Evaluation, vol. 6. New York: Plenum; 1987. 1075-1984.

Datta, S. K.; Schramm, R. E.; Abduljabbar, Z. Plate modes generated by EMATs for NDE of planar flaws. Thompson, D. O.; Chimenti, D. E., eds. Review of Progress in Quantitative Nondestructive Evaluation, vol. 6A. New York: Plenum; 1987. 101-108.

Datta, S. K.; Shah, A. H.; Ledbetter, H. M. Ultrasonic scattering and NDE of materials and cracks. Proceedings, ONR Symposium on Solid Mechanics Research for Quantitative NDE. Dordrecht, The Netherlands: Martinus Nijhoff; 1986. 361-376.

DelSanto, P. P.; Clark, A. V. Rayleigh wave propagation in deformed orthotropic materials. Thompson, D. O.; Chimenti, D. E., eds. Review of Progress in Quantitative Nondestructive Evaluation, vol. 5B, New York: Plenum; 1986. 1467-1414.

DelSanto, P. P.; Mignogna, R. B.; Clark, A. V.; Mitracović, D. Acousto-elastic determination of residual stresses. Proceedings, International Conference on Residual Stress; accepted.

deWit, R.; Fields, R. J. Wide plate crack arrest testing. Nucl. Eng. Des. 98: 194-155; 1987.

deWit, R.; Read, D. T.; Low, S. R., III; Harne, D. E.; McColskey, J. D.; Hicho, G. E.; Smith, L. C.; Danko, G.; Fields, R. J. Wide plate crack arrest testing: a description and discussion of the first two wide plate tests and the results of six, full thickness, bend bar tests. Interim report to the Naval Research Center. Nat. Bur. Stand. (U.S.) NBSIR; in press.

Glazer, J.; Morris, J. W., Jr.; Kim, S. A.; Austin, M. W.; Ledbetter, H. M. Temperature variation of the elastic constants of aluminum alloy 2090-T81. AIAA J. 25: 1271-1272; 1987.

Grong, O.; Siewert, T. A.; Edwards, G. R. Effects of deoxidation practice on the transformation behavior and toughness of steel welds. Weld. J. 65: 179-s-188-s; 1986.

Grong, O.; Siewert, T. A.; Martins, G. P.; Olson, D. L. A model for the silicon-manganese deoxidation of steel weld metals [86]. Metall. Trans. 17A: 1797-1807; 1987.

Heyliger, P. R.; Shull, P. J.; Moulder, J. C.; Gimple, M.; Auld, B. A. Numerical modeling of capacitive array sensors using the finite element method. Thompson, D. O.; Chimenti, D. E., eds. Review of Progress in Quantitative Nondestructive Evaluation. New York: Plenum; in press.

Hicho, G. E.; Brady, C. H.; Smith, L. C.; Fields, R. J. Effects of heat treatment on the mechanical properties and microstructures of four different heats of a precipitation hardening HSLA steel. J. Heat. Treat. 5: 7-19; 1987.

Hirth, J. P.; Lin, I. H. The thermodynamic force on line force defects. Philos. Mag. A. 56(1): 89-92; 1987.

Jones, E. R.; Datta, T.; Almasan, C.; Edwards, D.; Ledbetter, H. M. Low-temperature magnetic properties of fcc Fe-Cr-Ni alloys: Effects of manganese and interstitial carbon and nitrogen. Mater. Sci. Eng. 91:181-188; 1987.

Kasen, M. B. A strain-controlled torsional test method for screening the performance of composite materials at cryogenic temperatures. J. Mater. Sci.; accepted.

Kasen, M. B. High quality organic matrix composite specimens for research purposes. J. Compos. Technol. Res. 8(3): 103-106; 1986.

Kohn, G.; Siewert, T. A. The effect of power supply response characteristics on droplet transfer of GMA welds. David, S. A., ed. Advances in Welding Science and Technology. Metals Park, Ohio: Amer. Soc. Met.; 1986. 299-302.

Kriz, R. D.; Ledbetter, H. M. Elastic representation surfaces of unidirectional graphite-magnesium. San Antonio, Texas: Nondestructive Testing Information Analysis Center; Santa Barbara, California: Metal Matrix Composites Information Analysis Center; Columbus, Ohio: Metals and Ceramics Information Center; 1986. 63-76.

Kriz, R. D.; Ledbetter, H. M. Elastic-wave surfaces in anisotropic media. Huet, C., ed. Proceedings, 19th Annual Colloquium on Rheology of Anisotropic Materials; 1984 November 28-30; Paris, France. Toulouse, France: Cepadues; 1986. 79-91.

Kriz, R. D.; Sparks, L. L. Performance of alumina/epoxy thermal isolation straps. Clark, A. F.; Reed, R. P., eds. Accepted for publication in Advances in Cryogenic Engineering - Materials, vol. 34. New York: Plenum.

Ledbetter, H. M. Acoustoelastic residual-stress measurements: Role of anisotropic dislocation arrays. J. Appl. Phys.; accepted.

Ledbetter, H. M.; Austin, M. W. Deformed-polycrystalline-copper elastic constants. Phys. Status Solidi; forthcoming (1987 November).

- Ledbetter, H. M.; Austin, M. W. Internal strain (stress) in an SiC/Al particle-reinforced composite: An x-ray diffraction study. *Mater. Sci. Eng.* 89: 53-61; 1987.
- Ledbetter, H. M.; Austin, M. W. Molybdenum effect on volume in Fe-Cr-Ni alloys. *J. Mater. Sci.*; accepted.
- Ledbetter, H. M.; Datta, S. K. Effective elastic constants of materials with inclusions. Huet, C., ed. *Rheology of Anisotropic Materials*. Toulouse, France: Cepadues; 1986. 291-306
- Ledbetter, H. M.; Kim, S. A. Manganese contributions to the elastic constants of face-centered-cubic Fe-Cr-Ni stainless steel. *J. Mater. Sci.*; accepted.
- Ledbetter, H. M.; Kim, S. A. Molybdenum effect on Fe-Cr-Ni-alloy elastic constants. *J. Mater. Res.*; forthcoming.
- Lin, I.-H. Ductility improvement in particle reinforced aluminum composites: A ductile-fracture model based on void nucleation and growth. Yan, M. G.; Zhang, S. H.; Zheng, Z. M., eds. *Mechanical Behavior of Materials - V*. Oxford: Pergamon; 1987. 1261-1264.
- Lin, I.-H.; Thomson, R. M. The influence of dislocation density on the ductile-brittle transition in bcc metals. *Scr. Metall.* 20(10): 1367-1371; 1986.
- McCowan, C. N. Cryogenic Strength, Toughness, and Ferrite Content of Stainless Steel Welds. M.S. Thesis No. T 3349. Golden, Colorado: Colorado School of Mines; 1987.
- McCowan, C. N.; Siewert, T. A. Inclusions and fracture toughness in stainless steel welds at 4 K. Clark, A. F.; Reed, R. P., eds. *Advances in Cryogenic Engineering - Materials*, vol. 34. New York: Plenum; accepted.
- McCowan, C. N.; Siewert, T. A.; Reed, R. P.; Lake, F. B. Manganese and nitrogen in stainless steel SMA welds for cryogenic service. *Weld. J.* 66(3): 84s-92s; 1987.
- McCowan, C. N.; Siewert, T. A.; Tobler, R. L. Tensile and fracture properties of an Fe-18Cr-20Ni-0.16N fully austenitic weld metal at 4 K. *Trans. ASME* 108(4): 340-343; 1986.
- McHenry, H. I.; Purtscher, P. T.; Shives, T. R. Observations of hydrogen damage in a failed pressure vessel. *Corrosion Sci.*; in press.
- McHenry, H. I.; Read, D. T.; Shives, T. R. Failure analysis of an amine-absorber pressure vessel. *Mater. Perf.* 26(8): 18-24. 1987.
- Moulder, J. C.; Shull, P. J.; Capobianco, T. E. Uniform field eddy current probe: Experiments and inversion for realistic flaws. Thompson, D. O.; Chimenti, D. E., eds. *Review of Progress in Quantitative Nondestructive Evaluation*, vol. 6A. New York: Plenum; 1987. 601-610.



Nakajima, H.; Yoshida, K.; Shimamoto, S.; Tobler, R. L.; Purtscher, P. T.; Reed, R. P. Round robin tensile and fracture test results for an Fe-22Mn-13Cr-5Ni austenitic stainless steel at 4 K. Clark, A. F.; Reed, R. P., eds. Advances in Cryogenic Engineering - Materials, vol. 34. New York: Plenum; accepted.

Ogata, T.; Ishikawa, K.; Reed, R. P.; Walsh, R. P. Loading rate effects on discontinuous deformation in load-control tensile tests. Clark, A. F.; Reed, R. P., eds. Advances in Cryogenic Engineering - Materials, vol. 34. New York: Plenum; accepted.

Ogata, T.; Ishikawa, K.; Yuri, T.; Tobler, R. L.; Purtscher, P. T.; Reed, R. P.; Shoji, T.; Nakano, K.; Takahashi, H. Effects of specimen size and precracking temperature on  $J_{IC}$  test results for AISI 316LN at 4 K. Clark, A. F.; Reed, R. P., eds. Advances in Cryogenic Engineering - Materials, vol. 34. New York: Plenum; accepted.

Pugh, C. E.; Naus, D. J.; Bass, B. R.; Nanstad, R. K.; deWit, R.; Fields, R. J.; Low, S. R., III. Wide-plate crack-arrest tests utilizing a prototypical pressure vessel steel. Int. J. Pressure Vessel and Piping; in press.

Purtscher, P. T. Absence of stretch zones in austenitic stainless steels fractured at cryogenic temperatures. ASTM J. Test. Eval. 15(5): 296-298; 1987.

Purtscher, P. T.; Read, D. T. Effect of prior deformation on the 76-K fracture toughness of AISI 304L and AWS 208L stainless steels. ASTM J. Eng. Mater. Technol. 109: 151-157; 1987.

Purtscher, P. T.; Reed, R. P.; Read, D. T. Effect of void nucleation on fracture toughness of high-strength austenitic steels. ASTM STP. Philadelphia: Amer. Soc. Test. Mater.; in press.

Purtscher, P. T.; Walsh, R. P.; Reed, R. P. Modification of 316LN-type alloys. Clark, A. F.; Reed, R. P., eds. Advances in Cryogenic Engineering - Materials, vol. 34. New York: Plenum; accepted.

Purtscher, P. T.; Walsh, R. P.; Reed, R. P. Fracture behavior of 316LN tensile specimen at cryogenic temperatures. Clark, A. F.; Reed, R. P., eds. Advances in Cryogenic Engineering - Materials, vol. 34. New York: Plenum; accepted.

Read, D. T. J-integral values for small cracks in steel panels. ASTM STP. Philadelphia: Amer. Soc. Test. Mater.; in press.

Read, D. T. Strain Hardening and Stable Tearing Effects in Fitness-for-Service Assessment: First Interim Progress Report. Nat. Bur. Stand. (U.S.) NBSIR 86-3045; 1986.

Read, D. T.; McHenry, H. I. Post-weld Heat-Treatment Criteria for Repair Welds in 2-1/4Cr-1Mo Steel Superheater Headers: An Experimental Study. Nat. Bur. Stand. (U.S.) NBSIR 87-3075. 1987.

Read, D. T.; McHenry, H. I.; Petrovski, B. Elastic plastic models of surface cracks in tensile panels. Optical Methods in Composites. Bethel, Connecticut: Soc. Exper. Mech.; 1986 October. 210-216.

Reed, R. P. Austenitic stainless steels, with emphasis on strength at low temperatures. Walters, John, ed. Chapter in Alloying. Metals Park, Ohio: American Society for Metals; accepted.

Reed, R. P., ed. Materials Studies for Magnetic Fusion Energy Applications at Low Temperatures - X. Nat. Bur. Stand. (U.S.) NBSIR 87-3067; 1987 May; 438 pp.

Reed, R. P.; Simon, N. J.; Purtscher, P. T.; Tobler, R. L. Alloy 316LN for low temperature structures: A summary of tensile and fracture data. Proceedings, Eleventh International Cryogenic Engineering Conference. London: Butterworth Scientific; 1986. 786-790.

Reed, R. P.; Walsh, R. P. Tensile strain rate effects in liquid helium. Clark, A. F.; Reed, R. P., eds. Advances in Cryogenic Engineering - Materials, vol. 34. New York: Plenum Press; accepted.

Reed, R. P.; Walsh, R. P.; Fickett, F. R. Effects of grain size and cold rolling on the low temperature tensile properties and electrical resistivity of copper. Clark, A. F.; Reed, R. P., eds. Advances in Cryogenic Engineering - Materials, vol. 34. New York: Plenum; accepted.

Reno, R. C.; Clark, A. V.; Blessing, G. V.; Fields, R. J.; Govada, A.; Thompson, R. B.; DelSanto, P. P.; Mignogna, R. B.; Smith, J. F. Use of neutron pole figures to calibrate ultrasonic techniques for on-line texture control of aluminum plates. Wadley, H. N. G.; Rath, B. B.; Wolf, S. M.; Parrish, P. A., eds. Proceedings, Conference on Intelligent Processing of Materials and Advanced Sensors. Metals Park, Ohio: Amer. Soc. Met.; in press.

Reno, R. C.; Fields, R. J.; Clark, A. V. Crystallographic texture in rolled aluminum plates: neutron pole figure measurements. Thompson, D. O.; Chimenti, D. E., eds. Review of Progress in Quantitative Nondestructive Evaluation. New York: Plenum; in press.

Schramm, R. E.; Clark, A. V., Jr.; Mitracović, D. V.; Shull, P. J. Flaw detection in railroad wheels using Rayleigh-wave EMATs. Thompson, D. O.; Chimenti, D. E. eds. Review of Progress in Quantitative Nondestructive Evaluation, vol. 7. New York: Plenum; accepted.

Schramm, R. E.; Siewert, T. A. Sizing canted flaws in weldments using low-frequency EMATs. Thompson, D. O.; Chimenti, D. E., eds. Review of Progress in Quantitative Nondestructive Evaluation, vol. 6B. New York: Plenum, 1987. 1731-1736.

Scull, L. L.; Reed, R. P. Tensile and fatigue-creep properties of a copper-stainless steel laminate. Clark, A. F.; Reed, R. P., eds. Advances in Cryogenic Engineering - Materials, vol. 34. New York: Plenum; accepted.



Scull, L. L.; Sparks, L. L.; Arvidson, J. M. Low temperature mechanical property and thermal expansion measurements of silica aerogel foam. Clark, A. F.; Reed, R. P., eds. Advances in Cryogenic Engineering - Materials, vol. 34. New York: Plenum; accepted.

Shimada, M.; Tobler, R. L.; Shoji, T.; Takahashi, H. Size, side-grooving, and precracking effects on  $J_{IC}$  data for an SUS 304 stainless steel. Clark, A. F.; Reed, R. P., eds. Advances in Cryogenic Engineering - Materials, vol. 34. New York: Plenum; accepted.

Shull, P. J.; Capobianco, T. E.; Moulder, J. C. Design and characterization of uniform field eddy current probes. Thompson, D. O.; Chimenti, D. E. Review of Progress in Quantitative Nondestructive Evaluation, vol. 6A. New York: Plenum; 1987. 695-704.

Shull, P.; Heyliger, P.; Moulder, J. C.; Gimple, M.; Auld, B. A. Applications of capacitive array sensors to nondestructive evaluation. Thompson, D. O.; Chimenti, D. E. Review of Progress in Quantitative Nondestructive Evaluation, vol. 7. New York: Plenum; accepted.

Siewert, T. A.; Gorni, D.; Kohn, G. High-energy beam welding of type 316LN stainless steel for cryogenic applications. Clark, A. F.; Reed, R. P., eds. Advances in Cryogenic Engineering - Materials, vol. 34. New York: Plenum; accepted.

Siewert, T. A.; Schramm, R. E. Compressive stress effects on the ultrasonic detection of cracks in welds. Thompson, D. O.; Chimenti, D. E., eds. Review of Progress in Quantitative Nondestructive Evaluation, vol. 6B. New York: Plenum, 1987. 1593-1600.

Siewert, T. A.; Trevisan, R. E.; Purtscher, P. T. Fusion line shape versus toughness in HY-80 GMA welds. Nat. Bur. Stand. (U.S.) NBSIR 86-3043; 1986. 43pp.

Siewert, T. A.; Ziegenfuss, H. G. Welding in the Soviet Union - A closer view. Weld. J. 66: 27-34; 1987.

Simon, N. J.; Reed, R. P. Design of 316LN-type alloys. Clark, A. F.; Reed, R. P., eds. Advances in Cryogenic Engineering - Materials, vol. 34. New York: Plenum; accepted.

Simon, N. J.; Reed, R. P. Strength and toughness of AISI 304 and 316 at 4 K. J. Nucl. Mater. 141-143: 44-48; 1986.

Takahashi, H.; Shoji, T.; Tobler, R. L. Acoustic emission and its applications to fracture studies of austenitic stainless steels at 4 K. Clark, A. F.; Reed, R. P., eds. Advances in Cryogenic Engineering - Materials, vol. 34. New York: Plenum; accepted.

Tobler, R. L.; Reed, R. P. Proposed standard method for tensile testing of structural alloys at liquid helium temperatures. Reed, R. P., ed. Materials Studies for Magnetic Fusion Energy Applications at Low Temperatures - X. Nat. Bur. Stand. (U.S.) NBSIR 87-3067; 1987. 387-404.

Tobler, R. L.; Reed, R. P. Proposed standard method for fracture toughness testing of structural alloys at liquid helium temperatures. Reed, R. P., ed. Materials Studies for Magnetic Fusion Energy Applications at Low Temperatures - X. Nat. Bur. Stand. (U.S.) NBSIR 87-3067. 1987. 405-421.

Tobler, R. L.; Shoji, T.; Takahashi, H.; K. Ohnishi Fracture, acoustic emission, and adiabatic heating of austenitic stainless steels at liquid helium temperatures. Proceedings, Symposium on Acoustic Emission. Yamaguchi, K; Aoki, K.; Kishi, T., eds. The Japanese Society of NDI; 1986. 453-461.

Tobler, R. L.; Trevisan, R. E.; Siewert, T. A.; McHenry, H. I.; Purtscher, P. T.; McCowan, C. N.; Matsumoto, T. Strength, fatigue, and toughness properties of an Fe-18Cr-16Ni-6.5Mn-2.4Mo fully austenitic SMA weld at 4 K. Clark, A. F.; Reed, R. P., eds. Advances in Cryogenic Engineering - Materials, vol. 34. New York: Plenum; accepted.

Yoshida, K.; Nakajima, H.; Oshikiri, M.; Tobler, R. L.; Shimamoto, S.; Miura, R.; Ishizaka, J. Mechanical tests of large specimens at 4 K. Clark, A. F.; Reed, R. P., eds. Advances in Cryogenic Engineering - Materials, vol. 34. New York: Plenum; accepted.

SELECTED TECHNICAL AND PROFESSIONAL COMMITTEE LEADERSHIP

Advanced Materials Institute

1987 National Conference Committee

R. P. Reed

American Society for Metals

Joining Division

T. A. Siewert, Government Liaison

American Society for Testing and Materials

E24: Fracture Testing Committee

Proceedings, 18th National Symposium on Fracture Mechanics

D. T. Read, R. P. Reed, editors

E24.05: Terminology

R. deWit, Secretary

E24.06: Fracture Mechanics Applications

E24.06.04: Weld Testing

H. I. McHenry, Chairman

E28: Mechanical Testing

E28.04: Tension Testing

E28.04.03: Verification of Alignment

B. W. Christ, Chairman

E28.06: Hardness

E28.06.07: Hardness Test Block Intercomparison Task Group

T. R. Shives, Chairman

American Welding Society

Technical Papers Committee

T. A. Siewert

Welding Journal

T. A. Siewert, Reviewer

American Welding Institute

On-line Welding Data Base Committee

T. A. Siewert

Colorado School of Mines

Steel Research Institute Advisory Board

R. P. Reed

Federal Railroad Administration

Railroad Tank Car Safety Task Force

R. J. Fields, G. E. Hicho

International Cryogenic Materials Conference

Board of Directors

R. P. Reed, Finance Officer

International Cryogenic Materials Conference, continued  
Proceedings

R. P. Reed, Coeditor  
1987 Conference Program Committee  
M. B. Kasen

Mechanical Failures Prevention Group

T. R. Shives, Executive Secretary  
S. R. Low, Committee member  
T. R. Shives, Proceedings Editor

Metals Properties Council

Technical Advisory Committee  
R. P. Reed, B. W. Christ  
Materials for Utilization at Cryogenic Temperatures Task Group  
M. B. Kasen

Metallurgical Transactions

Board of Review  
H. M. Ledbetter

NBS-Boulder Editorial Review Board

R. L. Tobler

National Academy of Science

Materials Advisory Group of the Marine Board  
T. A. Siewert

Society of Automotive Engineers

1987 Symposium: Durability by Design  
B. W. Christ, cochairman of symposium

U.S. Department of Energy

Fossil Energy Research Review Panel  
R. J. Fields

U.S. Department of Energy, Office of Fusion Energy  
Analysis and Evaluation Task Group

N. J. Simon  
Joint U.S.-Japanese Exchange Program Advisory Committee  
H. I. McHenry, R. P. Reed  
Low-Temperature Materials for Magnetic Fusion Energy Committee  
R. P. Reed, Coordinator

U. S. Department of Transportation

Technical Hazardous Liquid Pipeline Safety Standards Committee  
R. J. Fields

Versailles Project on Advanced Materials and Standards Task Group  
Cryogenic Structural Materials Working Group  
R. P. Reed

Welding Research Council  
Data Base Task Group  
T. A. Siewert  
Materials and Welding Procedures Subcommittee  
T. A. Siewert



## INDUSTRIAL AND ACADEMIC INTERACTIONS

### Industrial Interactions

In response to requests from designers in industry, members of our division have supplied data and references on properties of specific materials and advice on material selection, data interpretation, measurement techniques, and welding procedures. Our expertise has been utilized in wind tunnel design, space instrumentation, accelerator design, cryogenic tankage, aerospace, and advanced aircraft applications. We are a major source of materials data at cryogenic temperatures. We provide handbook data on the cryogenic properties of stainless steels, copper, and copper alloys to many industries. Our excellent test facilities are often used by industrial personnel. These small requests, too numerous to be listed individually, accrue to a significant assistance to industry.

#### Aluminum Die-Casting Institute

The division is determining the shear and tensile properties of a newly developed die-casting alloy for the Aluminum Die-Casting Institute. Test specimens are provided by the die-casting industry, and some testing equipment is being loaned to NBS by Bell Laboratories for this work. The results will be disseminated through ASTM. Additional research on the fatigue properties of this new alloy is under way.

#### Amax Materials Research Center

H. M. Ledbetter is studying the elastic constants of pure molybdenum for Amax Materials Research Center in Ann Arbor, Michigan. This material can undergo low-temperature magnetic transitions that may affect the elastic constants of Fe-Cr-Ni-Mo alloys.

#### American Association of Railroads

The NDE group is collaborating with the American Association of Railroads on the design of ultrasonic systems for nondestructive evaluation of railroad wheels. Eventually these systems will be used for on-line inspection in railroad yards.

#### American Welding Institute

The division provided assistance to the American Welding Institute (AWI) during its formative period. The purpose of the organization is to improve the transfer of the latest welding technology to U.S. industry. Last year NBS and AWI hosted a workshop on Computerization of Welding Data to determine the best organization of data for increasing industrial productivity. Results of the workshop are guiding the development of a national welding data base.

#### Ball Aerospace

M. W. Austin measured the thermal expansivity of beryllium, which is used in the design of laser mirrors at Ball Aerospace; this information is essential for attaining maximum dimensional stability in the mirrors.

#### Combustion Engineering

As a major producer of nuclear power plants, Combustion Engineering (CE) has an ongoing interest in nuclear pressure vessel integrity. Heavy-section steel plate has been supplied by CE for characterization by NBS test methods. The behavior of these plates will be compared with the behavior of pressure vessel steels provided by Oak Ridge National Laboratory (ORNL). ORNL has machined the CE plates and included them in the ongoing program at NBS. NBS will provide dynamic crack growth, arrest, and fracture behavior information to CE for design and evaluation purposes.

#### Hercules Aerospace and Morton Thiokol

The NDE Group has initiated a collaboration with researchers at Hercules Aerospace and at Morton Thiokol on nondestructive evaluation of composites. Both electromagnetic and acoustical sensors will be tested for sensitivity to structural defects in composites. In addition, acoustical arrays will be fabricated for material property determination.

#### MTS Corporation

At the request of the MTS Corporation in Minneapolis, J. D. McColskey worked six weeks assisting the Société Européen Aérospatiale in Paris, France to set up a state-of-the-art million-dollar laboratory for cryogenic materials testing, particularly their closed-loop servo-hydraulic fatigue machines that are comparable to the ones in our laboratory.

#### Materials Research and Engineering

Several members of our division helped Materials Research and Engineering in Boulder, Colorado to establish standard test procedures for determining fatigue and fracture properties of materials at cryogenic temperatures.

#### Micromotion

H. M. Ledbetter and S. A. Kim measured the elastic constants of rods of five commercial alloys. Micromotion in Boulder, Colorado needed these measurements for the development of equipment to measure acoustic-elastic properties of metal tubes.

#### Perkin Elmer

H. M. Ledbetter is studying the sound velocities, thermal expansivity, and electrical resistivity of pure beryllium at low temperatures for Perkin Elmer in Danbury, Connecticut. Initial sound-velocity results suggest an unexpected low-temperature transition.

#### Potomac Electric Power Company

The division has performed numerous failure analyses for the Potomac Electric Power Company (PEPCO) for two reasons: (1) to assist the public utility in its service to the community and (2) to maintain and upgrade NBS competence in materials technology for the electric power industry. As the average age of U.S. plants increases and failures become more frequent, such competence will be needed to identify and transfer state-of-the-art technology to industry.

#### Rockwell International

A major low-temperature test program is in progress to measure the mechanical properties of selected titanium alloys, which are the main structural material for aerospace containers of liquefied hydrogen. The effects of different thermomechanical processes on the mechanical properties of these alloys at 20 K are being examined. Research has concentrated on tensile and notch tensile measurements of Ti-5Al-2.5Sn at 20 K, low-temperature elastic constants of Ti-Al-Sn alloys, and low- and high-cycle fatigue at 20 K. Distinctions between testing in gaseous and liquid cryogenic environments have been studied.

#### SCM Metal Products

H. M. Ledbetter is studying the elastic constants of alumina-dispersion-strengthened copper that is manufactured at SCM Metal Products in Cleveland, Ohio. Because the alumina particles are so small (a few hundred angstroms), modeling this material presents an intriguing problem.

#### Welding Research Council

The Welding Research Council (WRC) and NBS have established a joint program to produce nationally recognized weld procedures. The WRC is producing a series of welds that are representative of production welds. These welds, sectioned according to fabrication code requirements, are sent to NBS, which is serving as a nationally known, impartial testing laboratory capable of meeting the many accuracy and calibration requirements. NBS support for this program has increased from the testing of 200 specimens in 1985 to testing more than 1000 specimens in 1987. The WRC is currently reviewing the data from these tests and preparing the first weld procedure specifications. Eventually, these specifications will eliminate the costly and time-consuming individual tests for structural integrity that are now required of welding contractors.

#### Joint Industrial and Academic Interactions

##### Aluminum Company of America and Iowa State University

The NDE Group has worked with researchers of the Aluminum Company of America and the Ames Center for Nondestructive Evaluation at Iowa State University on ultrasonic monitoring of texture and formability in rolled aluminum alloy sheets.

## Academic Interactions

### Davidson College

H. M. Ledbetter collaborates with L. S. Cain of the Physics Department at Davidson College in Davidson, North Carolina in experimental studies of elastic constants. The high-temperature elastic-constant studies of L. S. Cain complement the low-temperature studies of H. M. Ledbetter. Currently, they are studying the carbon-plus-nitrogen alloying effects on Fe-Cr-Ni-alloy elastic constants, which are different at different temperatures.

### Lehigh University

G. E. Hicho collaborated with G. Sih, Head of the Fracture Mechanics Institute at Lehigh University in Bethlehem, Pennsylvania, on thermal effects at crack tips, a subject of ongoing research in the division.

R. J. Fields continued his work with T. Delph on the quantification of creep damage. R. J. Fields developed techniques for characterizing the population of cavities on the fracture surfaces of copper bicrystals that were tested at Lehigh. Comparison with various theories is under way.

### Pennsylvania State University

T. A. Siewert is working with S. Liu of Pennsylvania State University in the study of droplet transfer frequency in welding arcs. This study is revealing the physical basis for qualitative descriptions of the voltage and current values that produce acceptable welds. Arc extinction and reignition patterns determine the arc stability and so the weld spatter, one measure of an acceptable weld.

### Princeton University

The welding group is determining the strength of welds in copper alloys at 76 K and room temperature. Princeton Plasma Physics Laboratory requires the data for the design of the Compact Ignition Tokamak.

Several members of the division collaborated with G. Brown of the Princeton Plasma Physics Laboratory in research on the compressive mechanical properties of a nickel-alloy-copper laminate for possible use in fusion reactor magnet windings. The NBS 52-MN testing facility was used to perform static and cyclic loadings of these laminate specimens. More than ten thousand cycles were applied at loads between 15 and 20 MN in the first fatigue testing application for this NBS test equipment.

### Stanford University

The NDE group has continued collaboration with B. A. Auld of Stanford University in the area of electromagnetic sensors. Work this year centered on the comparison of theoretical and experimental results for characterization of a capacitive-array sensor.



#### Tohoku University

H. M. Ledbetter collaborates with Y. Shindo of the Mechanical Engineering Faculty on problems of waves scattered by interfaces. They use a scattered-plane-wave ensemble-average model.

#### University of Arkansas

H. M. Ledbetter, M. W. Austin, and S. A. Kim collaborate with A. M. Hermann of the Physics Department on the physical properties of the new high-critical-temperature metal-oxide superconductors. These properties include electrical resistivity, magnetic susceptibility, elastic constants, and crystal structure (by x-ray diffraction). The studies focus on substituting various trivalent rare-earth cations (R) in the compound  $R_1Ba_2Cu_3O_{7-x}$ .

#### University of California

The Physical Properties Group worked with J. Glazer and J. W. Morris, Jr. in studying the low-temperature constants of an Al-Li alloy.

#### University of Cambridge

H. M. Ledbetter works with P. Withers and M. Stobbs of the Metallurgy and Materials Science Department on the theoretical problem of internal stress in composites, stress that arises from differences in the thermal expansivities of the particle and matrix components.

#### University of Colorado

H. M. Ledbetter collaborates with T. Datta of the Physics Department on theoretical and experimental studies of low-temperature austenitic-steel physical properties, especially elastic constants and magnetic susceptibility. In these materials, physical properties (and perhaps plastic-deformation properties) depend on the magnetic state. They also study the elastic and magnetic properties of the new high-critical-temperature metal-oxide superconductors, especially  $Y_1Ba_2Cu_3O_{7-x}$ , which show large elastic and magnetic changes at the critical temperature.

H. M. Ledbetter collaborates with R. Edge of the Physics Department on studies of the low-temperature magnetic state in Fe-Cr-Ni alloys. Recently, at Oak Ridge National Laboratory, they obtained new neutron-diffraction results, which they are now trying to interpret.

#### University of Stuttgart

H. M. Ledbetter collaborates with E. Kröner and B. K. D. Gairola on the theoretical problems of the elastic constants of polycrystals. This year, they calculated the elastic constants of perfectly random polycrystalline graphite. These new results help to explain the peculiar elastic behavior of two important technological materials: graphite fibers (used in composites) and cast iron.



Vanderbilt University

T. A. Siewert collaborated with M. E. Shepard and G. E. Cook in modeling the self-regulation process in gas-metal-arc welding. Precise measurements of arc length, obtained in the NBS welding laboratory, are being used to determine the coefficients in the model.



# APPENDIX



# **Institute for Materials Science and Engineering**

**L. H. Schwartz, Director**

**R. B. Johnson, Associate Director**

## **Nondestructive Evaluation**

**H. T. Yolken, Chief**  
**L. Mordfin, Deputy**

## **Institute Scientists**

**J. W. Cahn**  
**R. M. Thomson**

## **Metallurgy**

**E. N. Pugh, Chief**  
**J. H. Smith, Deputy**

## **Polymers**

**L. E. Smith, Chief**  
**B. M. Fanconi, Deputy**

## **Ceramics**

**S. M. Hsu, Chief**  
**S. J. Dapkunas**

## **Fracture and Deformation**

**H. I. McHenry, Chief**

## **Reactor Radiation**

**R. S. Carter, Chief**  
**T. M. Raby, Deputy**



```

graph TD
    A["DIRECTOR  
Deputy Director  
Office of Congressional and Legislative Affairs  
Associate Director for International and Academic Affairs  
Associate Director for Industry and Standards"]
    B["ASSOCIATE DIRECTOR FOR PROGRAMS, BUDGET, & FINANCE  
Program Office  
Budget Office  
Office of the Comptroller"]
    C["OFFICE OF THE DIRECTOR NBS/BOULDER LABORATORIES"]
    D["DIRECTOR OF ADMINISTRATION  
EEO Support  
Information Resources & Services  
Public Information Management Systems  
Plant Facilities Services  
Occupational Health & Safety  
Personnel Acquisition and Assistance"]
    E["NATIONAL MEASUREMENT LABORATORY  
Office of Standard Reference Data  
Office of Measurement Services  
Center for Basic Standards  
Center for Radiation Research  
Center for Chemical Physics  
Center for Analytical Chemistry"]
    F["NATIONAL ENGINEERING LABORATORY  
Center for Applied Mathematics  
Center for Electronics & Electrical Engineering  
Center for Manufacturing Engineering  
Center for Building Technology  
Center for Fire Research  
Center for Chemical Engineering"]
    G["INSTITUTE FOR COMPUTER SCIENCES & TECHNOLOGY  
Information Systems Engineering Division  
Systems and Software Technology Division  
Computer Security Division  
System and Network Architecture Division  
Advance Systems Division"]
    H["INSTITUTE FOR MATERIALS SCIENCE & ENGINEERING  
Office of Nondestructive Evaluation  
Ceramics Division  
Fracture and Deformation Division  
Polymers Division  
Metallurgy Division  
Reactor Radiation Division"]

    A --- B
    A --- C
    A --- D
    A --- E
    A --- F
    A --- G
    A --- H
  
```

U.S. DEPT. OF COMM. <b>BIBLIOGRAPHIC DATA SHEET</b> (See instructions)		1. PUBLICATION OR REPORT NO. NBSIR 87 3613	2. Performing Organ. Report No.	3. Publication Date
4. TITLE AND SUBTITLE Institute for Materials Science and Engineering Fracture and Deformation Division Technical Activities 1987				
5. AUTHOR(S)				
6. PERFORMING ORGANIZATION (If joint or other than NBS, see instructions)  NATIONAL BUREAU OF STANDARDS DEPARTMENT OF COMMERCE WASHINGTON, D.C. 20234			7. Contract/Grant No.	
			8. Type of Report & Period Covered	
9. SPONSORING ORGANIZATION NAME AND COMPLETE ADDRESS (Street, City, State, ZIP) Fracture and Deformation Division, 430 National Bureau of Standards 325 Broadway Boulder, CO 80303				
10. SUPPLEMENTARY NOTES  <input type="checkbox"/> Document describes a computer program; SF-185, FIPS Software Summary, is attached.				
11. ABSTRACT (A 200-word or less factual summary of most significant information. If document includes a significant bibliography or literature survey, mention it here)  This report summarizes the 1987 fiscal-year programs of the Fracture and Deformation Division of the Institute for Materials Science and Engineering. Its two major programs are Elastic-Plastic Fracture Mechanics and Fracture Mechanisms and Analysis. Elastic-Plastic Fracture Mechanics includes nondestructive evaluation, welding, and thermomechanical processing. Fracture Mechanisms and Analysis consists of physical properties, fracture physics, composite mechanics, cryogenic materials, and material performance. The report summarizes the principal accomplishments in these research areas, including wide-plate crack-arrest tests, a new model of plastic fracture, design and evaluation of an capacitive-array probe, measurement of the natural frequency for short-circuiting transfer in gas-metal-arc welding, and a model for prediction of the elastic properties of porous ceramics.  The report lists the division's professional staff, their research areas, publications, leadership in professional societies, and collaboration in research programs with industries and universities.				
12. KEY WORDS (Six to twelve entries; alphabetical order; capitalize only proper names; and separate key words by semicolons) austenitic steels; composites; deformation; fracture mechanics; fracture physics; low temperatures; nondestructive evaluation; physical properties; welding				
13. AVAILABILITY <input checked="" type="checkbox"/> Unlimited <input type="checkbox"/> For Official Distribution. Do Not Release to NTIS <input type="checkbox"/> Order From Superintendent of Documents, U.S. Government Printing Office, Washington, D.C. 20402. <input checked="" type="checkbox"/> Order From National Technical Information Service (NTIS), Springfield, VA. 22161			14. NO. OF PRINTED PAGES 80  15. Price \$13.95	









**IR 87-3614**

**CANCELLED**

**NOT AVAILABLE FOR BINDING**







